

**THE PHYLOGENETICS AND POPULATION GENOMICS OF CRYPTIC LINEAGES
OF MASSIVE *PORITES* ON GUAM**

BY
Karim D. Primov

A thesis submitted in partial fulfillment of the
requirements for the degree of

MASTER OF SCIENCE
IN
BIOLOGY

SUPERVISORY COMMITTEE

Dr. David Combosch, Chair

Dr. Sarah Lemer

Dr. Peter Houk

Dr. Zac Forsman

UNIVERSITY OF GUAM
DECEMBER 2020

TO THE OFFICE OF GRADUATE STUDIES

The members of the committee approve the thesis of Karim Primov presented on December 2nd, 2020.

Dr. David Combosch, Chair

Dr. Sarah Lemer, Member

Dr. Peter Houk, Member

Dr. Zac Forsman, Member

ACCEPTED:

Troy McVey, Ed.D.
Director of Graduate Studies

Date

Table of Contents

Acknowledgements	4
Abstract	5
List of Figures	7
List of Tables	7
Introduction.....	8
Hypotheses:	11
Materials and Methods.....	12
Fieldwork.....	12
Lab work	13
Bioinformatics and Analyses.....	15
Results.....	19
Reads and Loci	19
Phylogenetic Analyses.....	19
Multi-locus genotyping and Clonality.....	23
Interspecific Genomic Analyses	24
Intraspecific Genomic Analyses	29
Symbiont Profile Characterization.....	31
Discussion	34
Phylogenetic Clade Comparisons.....	34
Symbionts	39
Conservation.....	40
Conclusions.....	41
Literature Cited	42
Supplementary Material	48

Acknowledgements

I would first like to thank my advisor, Dr. David Combosch, for taking me on as his first ever student. Over the course of working under him for almost 3 and a half years, our discussion about the literature and talks of potential new studies have really made me want to pursue a career in evolutionary biology. I had a lot of growing pains moving out to Guam, but he was always there to get me back on the right track, and I've learned so much about science and what it takes to be a research scientist, something that I am forever grateful for! I would also like to thank Dr. Sarah Lemer, Dr. Peter Houk, and Dr. Zac Forsman for taking the time to be on my committee. I've received tons of great feedback from them and am very happy that I'm in good hands to study *Porites* genomics, which has definitely been an enormous challenge. I also want to thank Dave Burdick for his work and assistance on micromorphological analysis of my thesis specimens! I would also like to thank Dr. Terry Donaldson, and Dr. Bastian Bentlage for their help over these past few years. I also want to thank Dr. Laurie Raymundo, who has been a huge help and has looked out for me over the past few years as well, and I'll be forever indebted to her for letting me live at the ML House! I want to thank Dr. Peter Glynn back at the University of Miami RSMAS so, so much for his mentorship during my undergraduate years and for recommending UOG as a place to do my master's degree. I am forever indebted to him and his wife, Mrs. Carmen, for all the guidance and support he has provided me since my undergrad. I can definitely say that I profited greatly from moving to Guam and have really enjoyed living on a tropical island with real coral reefs. I want to thank Dareon Rios for being the best lab partner I can possibly think of. I can't thank her enough for all the help and support she's given me over the past few years, and for even welcoming me to her family and getting me back on my feet after a week's worth of failed PCRs! I want to thank my dear friends Abram Townsend and Benjamin E. Deloso for keeping me sharp at Super Smash Bros., and for just being awesome friends from the beginning. We all look out for each other, I'm really, really glad I have you guys in my life. I also want to thank Coco Sartor, Andrew McInnis, Ka'ohinani Kawahigashi, Melissa Gabriel, and Mariel Cruz for helping me with fieldwork. I want to thank Jess Fernandez for her help with mitochondrial barcoding, and I'm glad the Island Evolution Lab has a charismatic person like you to carry on from what David, Dareon and I started. I also want to thank my former roommates over the past few years, Colin Lock and Kelsie Ebeling-Whited. It's definitely gotten hectic at times, but there've definitely been a lot of positives that came out of those times too. I also want to thank Matt Mills, who's made living at the ML House really chill and comfortable, even though we don't have the same taste in music. I want to thank my mom and Dad, George and Rachida, for being the best parents I could've possibly had. I've definitely been a handful for the past 26 years, but you two never gave up on me and I wouldn't want any other set of parents. I want to thank my sister Nadia for always being overprotective and having my best interests at heart. I'm super proud of her for becoming an elementary school teacher, something I know she's passionate about and will go very far in life if she continues in primary education. I want to also thank Uncle Jamal, Gina and Leila for making fun of Nadia every time you guys come to the house, and I also want to thank my family back in Morocco for always making me feel at home even though I don't speak Darija. I also want to thank my childhood friends Richard and Phillip Beauge, and the friends I've kept since college, Kritos Vasiloudes and Max McKoul for all the good times and laughs.

ABSTRACT OF THE THESIS of Karim Primov for the Master of Science in Biology presented December 2nd, 2020

Title: The Phylogenetics and Population Genomics of Cryptic Lineages of massive *Porites* on Guam

Approved:

Dr. David Combosch, Chair, Thesis Committee

One of the main coral genera on Guam's reefs is *Porites*, which includes an unresolved number of cryptic massive *Porites* species. Massive *Porites* can be found in multiple environments, from clear fore reefs to turbid river deltas. Higher bleaching resistance has been observed in marginal turbid environments compared to fore reef environments. Differential bleaching response may therefore be environmentally mediated or driven by local intra- or interspecific adaptations. In this study, I employ a ddRADSeq approach to identify both the extent of potential genetic differentiation and levels of genetic diversity of massive *Porites* in two different environments on Guam. I detected six phylogenetically distinct clades among massive *Porites* on Guam that likely constitute different species. Some of these correspond to previously recognized Indo-Pacific massive *Porites* species. The largest clade predominantly occurs in turbid river deltas and constitutes 75% of all analyzed massive *Porites* in river deltas. All other clades occur predominantly on fore reefs, with some found throughout the extent of Guam's fore reefs, while some are almost exclusively confined to a single location. Bleaching resistance of massive *Porites* in turbid environments may therefore be due to interspecific differences. The two largest clades exhibited no substructure around Guam, indicating high levels of connectivity, even among

discontinuous river deltas habitats. In addition, I found indications for clonality in the four largest clades in this study. The dominant algal symbiont among massive *Porites* on Guam was found to be *Cladocopium*, regardless of host identity or environment. However, *Durusdinium* and *Breviolum* were identified as secondary symbionts in fore reefs and river deltas, respectively. This study unveils cryptic diversity in an ecologically important reef builder. Conservation of cryptic massive *Porites* on Guam is therefore crucial to prevent the loss of local biodiversity in this foundational coral complex.

Keywords: massive *Porites*, ddRAD, phylogenetics, river deltas, fore reefs, conservation management

List of Figures

Figure 1: Map of Southern Guam fore reef and river delta populations; a map of the geographic extent of sampling of massive <i>Porites</i> on Guam (Credit: Google Earth).	14
Figure 2: 1000 bootstrap RAxML tree using 189,683 concatenated SNPs; corallite photographs of samples representing 4 massive <i>Porites</i> lineages	20
Figure 3: Genomic dataset PCoA	25
Figure 4: Genomic dataset K=4 NGSAdmix plot	27
Figure 5: Riverine and Oceanic clade PCoAs.	30
Figure 6: East Fore Reef Clade PCoA	30
Figure 7a-c: Clade-specific NGSAdmix K=2-4 plots for the Oceanic, Riverine and East Fore Reef clades	31
Figure 8: Proportions of four algal symbiont genera across samples from all clades	33
Figures 9: Mitochondrial DNA tree of Caribbean and Indo-Pacific <i>Porites</i> (Forsman et al., 2009)	34

List of Tables

Table 1: Sample count and percentage of samples in genomic analysis for all clades	23
Table 2: Per-clade distribution of samples by environment in each geographic location.	24
Table 3: GenoDive pairwise F_{ST} values calculated using	28
Table 4: Clade-specific population genetic summary statistics	28

Introduction

Coral cover and diversity are declining at unprecedented rates on a global scale due to both global and local stressors, which detrimentally impact reef-associated marine life (Bruno & Selig, 2007; Doney et al., 2012; Gardner, et al., 2005; Hoegh-Guldberg et al., 2007; T. P. Hughes et al., 2007). It is therefore crucial to protect and conserve coral reefs from degradation to prevent local extinction and loss of biodiversity of both ecologically and economically significant reef-building taxa. Marginal coral reefs, including turbid-zone reefs, have been identified as potential refuges for threatened marine taxa (de Oliveira Soares, 2020; Sully & van Woesik, 2020; Teixeira et al., 2019). This is because they can withstand the sub-optimal conditions found in these habitats, including pollution, fluctuations in salinity and temperature, and higher levels of turbidity and sedimentation (de Oliveira Soares, 2020; Guest et al., 2016; Loiola, et al., 2019; Porter & Schleyer, 2017). For example, there was up to 99% coral mortality in the Maldives during the 1998 ENSO, but lower than 50% mortality in Sulawesi, Southwest Sri Lanka, and Western Zanzibar, where reefs were located in turbid waters or upwelling locations (Goreau et al., 2016). More recently, there were no significant changes in coral cover, community structure, and partial pigmentation loss in turbid-zone reefs compared to the extensive bleaching and mortality observed in offshore reefs in the Paluma Shoals reef complex (Australia) during a 2015-2016 bleaching event (Morgan et al., 2017). Two environmental factors with notable influence on coral survival and resilience during bleaching events in turbid-zone river deltas are turbidity and heterotrophy, which massive *Porites* may be well-suited to survive in since few coral taxa are found in these marginal habitats.

Generally, turbidity caused by anthropogenic activity is detrimental for coral health and survival, preventing corals from receiving necessary light (Hodgson, 1990; Humanes et al., 2017; Pollock et al., 2014). In several cases, however, turbidity has been found to be beneficial for coral survival during bleaching events, buffering corals from high levels of solar radiation (Jokiel &

Brown, 2004; Morgan et al., 2017; Van Woesik et al., 2012). Moreover, heterotrophy has been found to provide the coral host with alternate sources of nutrients and carbon when the coral-zooxanthellae symbiosis is impaired during bleaching events. For example, Hughes & Grottoli, (2013) found that some corals can increase the amount of heterotrophic carbon incorporated into their tissues for almost a year following a bleaching event to compensate for their *Symbiodinium*'s reduced photosynthetic efficiency. The benefits of heterotrophy on coral survival, however, may vary by species and genera. For example, Grottoli et al., (2006) found that *Porites compressa* and *P. lobata* do not significantly increase heterotrophic feeding during bleaching events compared to *Montipora capitata*. In summary, moderate levels of turbidity in marginal reefs can mitigate the detrimental effects of harmful levels of irradiance on corals during bleaching events, while heterotrophy can provide turbid zone corals with alternate sources of nutrients, however, the benefits of heterotrophy vary among different coral taxa.

Differential bleaching response among coral taxa may be environmentally mediated or driven by interspecific or intraspecific genetic differences. For example, Hoogenboom et al., (2017) found lower levels of bleaching in staghorn *Acropora* on Lizard Island (Australia) in shaded microhabitats compared to those exposed to higher light levels. In another study, Frade et al., (2018) found significantly lower levels of bleaching and mortality in deep mesophotic reefs in the Great Barrier Reef (40% bleached at 40 m) compared to shallower reefs (60-69% bleaching at 5-25 m). Deep reefs, however, experienced severe bleaching, indicating that deep mesophotic reefs may provide more limited climate change refugia than previously considered (Bongaerts et al., 2017; Frade et al., 2018). Differential bleaching response has also been found to be driven by interspecific and intraspecific genetic differences. For example, Kenkel et al., (2013) found that nearshore *Porites asteroides* in the Florida Keys exhibited lower levels of bleaching compared to

offshore *P. asteroides* populations in the Florida Keys due to coral host population structure driven by differences in thermal regimes between sites. Identifying whether differential bleaching response is environmentally mediated, driven by interspecific or intraspecific genetic differences, or driven by a combination of both is critical in identifying and conserving resilient coral taxa that may be useful in the restoration of threatened, vulnerable coral reefs.

On Guam, *Porites* is one of the most prominent reef-building coral genera, including multiple massive *Porites* species (Myers & Raymundo, 2009). Massive *Porites* on Guam can be found in many different habitats, from fore reefs to river deltas, and includes *P. lobata*, *P. lutea*, *P. australiensis*, and *P. murrayensis*, among others (Horton et al., 2020; Randall, 2003). Massive *Porites* can be found in a variety of colors and are usually characterized by their notable mounding morphology (Horton et al., 2020). Massive *Porites*, however, are some of the most challenging coral species to identify, with respect to both gross morphological features and micromorphological features (Forsman et al., 2015; Forsman et al., 2017). This is especially the case for massive *Porites*, which have frequently been found to consist of multiple cryptic genetic lineages due to morphological convergence. For example, Terraneo et al., (2019) found that Red Sea *Porites* belonging to a single morphospecies belong to five distinct genetic clades. On the contrary, phenotypic plasticity has also been observed in *Porites*. For instance, Terraneo et al., (2019) also found in the same study that all specimens identified morphologically as *Porites annae*, *P. echinulata*, *P. lobata*, *P. lutea*, and *P. solida* group into one clade. In another study, an information theoretic analysis was found to provide no support to uphold Caribbean *Porites divaricata*, *P. furcata*, and *P. porites* as distinct species (Prada et al., 2014). Moreover, Forsman et al., (2009) and Forsman et al., (2017) failed to distinguish *Porites lobata* and *Porites compressa* as distinct species due to potential hybridization between these species. In a later study, however,

fixed differences were found between coral host and symbiont loci between both morphospecies, indicative of ongoing speciation (Forsman et al., 2020). These studies illustrate the difficulty in identifying massive *Porites*. Identifying the number of genetic clades of massive *Porites* on Guam, which may be overlooked in conservation management, merits further investigation.

In this study, I employ a double-digest RADSeq approach to determine if massive *Porites* on Guam in river deltas and fore reefs consists of either a single or multiple genetic clades. I also seek to determine if divergence is driven by either differences in environment or geographic separation. Finally, I aim to assess the genetic diversity and extent of gene flow among massive *Porites*, both around Guam and between these different environments.

Hypotheses:

- **Hypothesis 1:** massive *Porites* on Guam comprise one species with multiple, locally adapted populations.
- **Hypothesis 2:** River delta and fore reef massive *Porites* are genetically differentiated from one another due to adaptation to different environments.
- **Hypothesis 3:** Genetic diversity is higher in fore reef massive *Porites* due to the high connectivity and abundance of fore reef massive *Porites* on Guam.

Materials and Methods

Fieldwork

Guam is an island in the Western Pacific Ocean, approximately 2500 kilometers East of the Philippines and 2500 kilometers South of Tokyo, Japan. It is the southern-most island in the Marianas Island chain and is approximately 541 square kilometers large, with all river deltas confined to the Southern region of the island (Morton & Perry, 1999). Three Southern Guam river delta massive *Porites* populations were sampled at Inarajan, Talofofu Bay, and Fouha Bay. Adjacent fore reef populations were sampled at each site to determine the extent of differentiation and compare levels of genetic diversity of massive *Porites* in these two environments. An additional Northern fore reef population was sampled in Ritidian to determine the extent of gene flow and characterize genetic diversity among massive *Porites* throughout Guam's fore reefs.

Massive *Porites* identification in the field was based off photos and species descriptions from, ICUN, World Registry of Marine Species (WORMS), and Guam Reef Life. Specifically, only massive *Porites* colonies with coarse colony morphologies consistent with *Porites lutea* were sampled in this study. Sampling took place between 3-6 meters depth at each site using scuba diving and snorkeling, and 3-4 cm nubbins from each colony were collected using a hammer, chisel, and pliers. Colonies were sampled approximately 2-3 meters apart to avoid resampling previously connected tissue of the same colony. Fore reef populations were chosen based on both proximity to the nearby river delta and abundance of massive *Porites* and were sampled within a 50 x 50 m quadrat (Figure 1). River delta populations were sampled at the same depth along a 250 m transect starting at the closest colony to each river mouth (Figure 1). For each sample, a picture of the entire colony was taken, as well as a close-up and sample label picture. Samples were kept alive in sea water vials upon arrival at the UOG Marine Laboratory, where one half of each sample

nubbin was preserved in 70% ethanol and then frozen in a -20°C freezer. The remaining half was soaked in bleach and kept as a voucher specimen for future micromorphological analyses in the UOG biorepository, as shown in Figure 2b. Overall, two hundred and eighty samples were collected for this study, with forty samples collected from each population.

Lab work

DNA was extracted using the Qiagen Animal Blood and Tissue DNA extraction kit (Qiagen, Hilden, Germany) and the Epoch Mini Prep GenCatch extraction kit (Epoch Life Sciences, Inc., Missouri City, TX) following an optimized manufacturer's protocol. Specifically, extractions were eluted in half of the protocol's recommended elution volume to increase DNA concentration for sequencing preparation. After extraction, DNA quantity was measured for each sample using a Qubit High Sensitivity dsDNA fluorometer (Thermo Fischer Scientific, Waltham, MA). Libraries were generated using a modified version of the original double-digest RAD (ddRAD) protocol by Peterson et al., (2012) per Combosch et al., (2017). First, extracted DNA was digested using two restriction enzymes (PstI and MspI, New England BioLabs, Ipswich, MA). Digested DNA was then re-quantified and ligated to adaptors with sample-specific barcodes and primer annealing sites. Barcoded samples were then multiplexed into pooled libraries. DNA fragments were then size-selected (350-450 bp) on a 2% agarose gel using an Invitrogen E-gel (Invitrogen, Carsbad, CA). Size-selected libraries were then amplified using PCR (cycle: 30 seconds (98°C); 15-20 cycles [10 seconds (95°C), 30 seconds (65°C), 60 seconds (72°C)]; 5 minutes (72°C); 4°C) for 16, 18, and 20 cycles using combinations of P1 and P2 primers specific to each pooled library. Amplified libraries were then quantified using a Qubit High Sensitivity dsDNA fluorometer (Thermo Fischer Scientific, Waltham, MA) and an Agilent Bioanalyzer High

Sensitivity DNA assay (Agilent Technologies, Santa Clara, CA), and then sequenced using the Illumina NextSeq500 (Illumina, Inc., San Diego, CA) at the UOG Marine Laboratory.

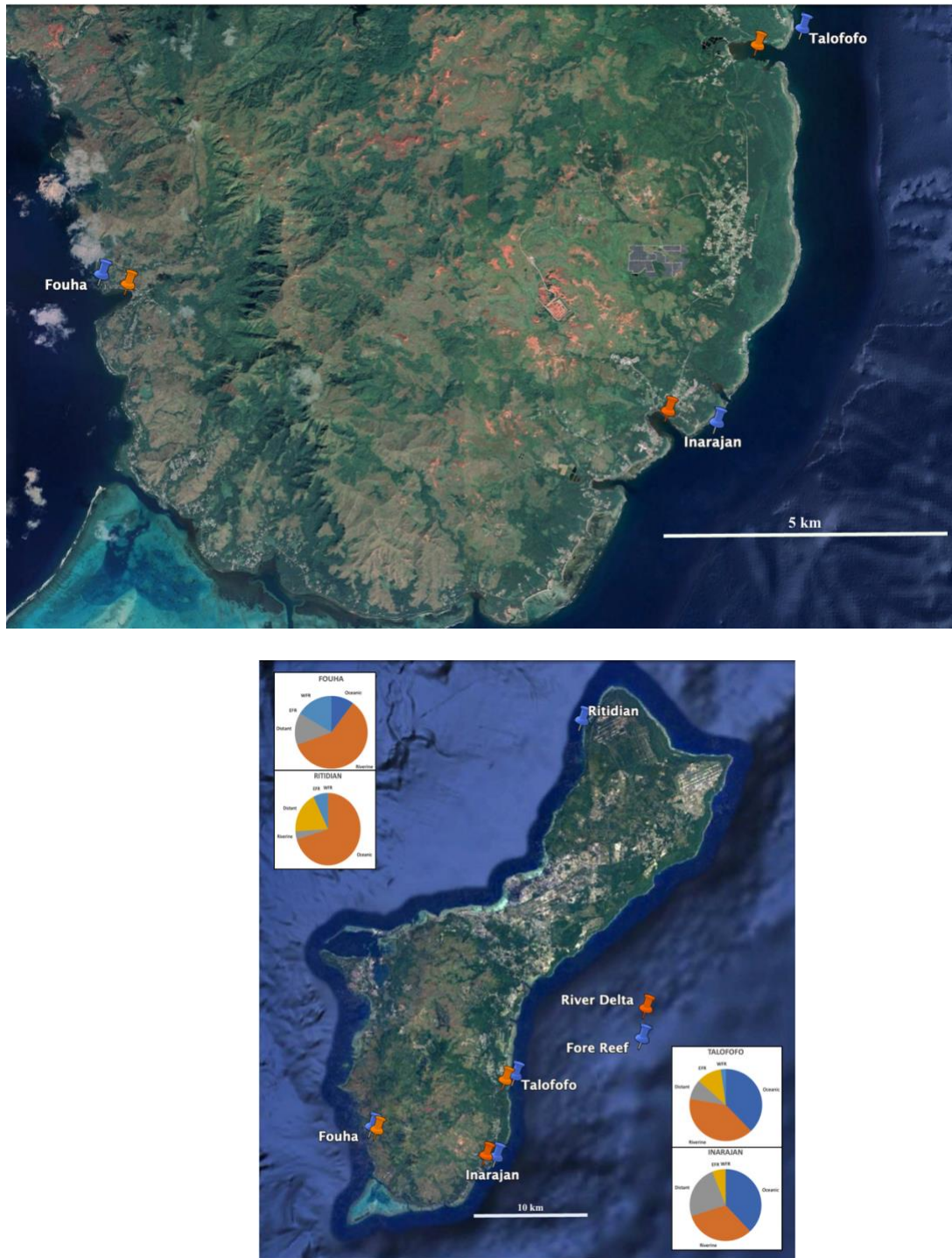


Figure 1: (a) Map of Southern Guam fore reef and river delta populations and (b) geographic extent of sampling of massive *Porites* on Guam (Credit: Google Earth).

Bioinformatics and Analyses

Quality Filtering

Raw sequence reads were first quality-trimmed using TrimGalore version 0.6.5 to remove any low-quality reads [filtered out low quality reads (--phred33, -q5), minimum read length of 20 bp (--length 20), adapter removal stringency(--stringency 1 -e 0.1)] or reads with uncalled SNPs and then demultiplexed using a custom made python3 script (Martin, 2011; H. Weigand, pers. comm). After barcode removal, reads were first aligned to the *Porites lutea* bacterial metagenome and then to *P. lutea*'s symbiont genome using Bowtie2 to remove non-coral loci (Langmead & Salzberg, 2012; Voolstra et al., 2015). In Bowtie2, sample-specific raw reads were sorted into either “aligned” or “unaligned” sample-specific folders after reference-aligning to the coral host, bacterial, and symbiont genomes. Reads that didn't match either of the two genomes were then aligned to the *P. lutea* coral host genome using Bowtie2 to generate filtered coral reads (Voolstra et al., 2015).

Multilocus genotyping and Dataset Curation

Aligned reads were converted to genotype data in two ways. First, genotype likelihoods were generated with the program ANGSD since genotype likelihood analyses are ideal for low-to medium-coverage sequence data (Korneliussen et al., 2014). ANGSD was run with the following filters: minimum mapping quality=20, minimum read quality=25, minimum minor allele frequency=0.05, minimum read depth per locus/individual=8. In addition, loci were only retained that were present in at least 80% of all included samples. Genotype likelihoods were used for clonality analyses, principal coordinate analyses (ngsconv) and admixture analyses (NGSAdmix). In addition, aligned reads were also converted to genotype calls using STACKS (Catchen, 2013; Catchen et al., 2011) using a reference-based approach, with SNPs identified using a maximum-

likelihood model. Furthermore, the STACKS populations program only retained loci that were present in both 30% and 80% of all samples. Genotype calls were used for the following analyses: RAxML phylogenetic analyses, pairwise F_{ST} , AMOVA, population genomic summary statistics. After multi-locus genotyping, two datasets were curated for phylogenetic and population genomic analyses. This is because population genomic analyses require a very dense, large data matrix to identify genome-wide population structure and diversity, whereas phylogenetic analyses can be performed using a sparser data matrix to infer the evolutionary relationships among closely related taxa.

Phylogenetic Analysis

Phylogenetic analysis was based on a concatenated, variable site sequence alignment of the phylogenetic dataset. Variable sites were used instead of entire sequences to enable SNP ascertainment bias correction. The variable site sequence alignment was generated using reference-aligned coral reads in the populations module in the program STACKS (Catchen, 2013). Phylogenetic analysis was conducted to infer the evolutionary relationship of massive *Porites* on Guam using a maximum-likelihood approach with RAxML 8.2.4 using the model GTRCAT on the CIPRES web portal with 1000 bootstrap replicates and SNP ascertainment bias correction (Miller et al., 2010).

Clonality

Clonality was assessed to remove replicate genotypes from the genomic dataset. Removal of clonal samples is crucial since clonal samples have a tendency to form distinct genetic clusters, altering results in further genomic analysis. Interestingly, clones have been recently reported for massive *Porites*, despite few studies investigating massive *Porites* clonality (Boulay et al., 2013; Brown et al., 2020). Clonal identification is non-trivial, however, since identical, clonal samples

may not be identified as such due to sequencing errors. Therefore, I used an identity-by-state (IBS) analysis following Manzello et al., (2019) and Barfield et al., (2020) to generate pairwise relatedness covariance matrices to identify clones. Relatedness dendrograms using the same covariance matrices were plotted in R to provide a visual of sample pair relatedness (Ihaka & Gentleman, 1996). Moreover, technical replicates were used to provide a minimum level of diversity among identical genotypes and to establish a clonal relatedness threshold to identify clonal samples. After clones were identified, the best sequenced sample of each genotype was retained for subsequent analyses.

Interspecific and Intraspecific Clade Analysis

The sample count and percent composition of all samples in each massive *Porites* lineage were calculated with respect to geographic distribution, environment, and color phenotype. to determine the fidelity of any massive *Porites* lineage to a specific geographic location or environment, and to determine whether color phenotype is a useful proxy for in-situ clade identification. All tables were generated using Microsoft Excel (Microsoft Office, Redmond WA) and are found in the supplementary material (Tables 1-6).

Principal coordinate analyses were performed with the ANGSD program `ngscover` (Korneliussen et al., 2014) to assess and visualize any differentiation of samples for all genotyped samples and for the two largest clades separately. Admixture analyses were performed with the ANGSD subprogram `NGSAdmix` (Korneliussen et al., 2014) to determine the most parsimonious number of genetic clusters found in the entire genomic dataset and for the three largest clades separately. Population genetic summary statistics that measure levels of genetic diversity and extent of inbreeding, including observed and expected heterozygosity, as well as nucleotide diversity, percentage of polymorphic loci, and inbreeding coefficients, are reported for STACKS.

None of these statistics were corrected for sample size bias in STACKS. In addition, pairwise F_{ST} s were calculated using genotype calls in GenoDive to obtain p-values that cannot be calculated using genotype likelihoods.

The proportions of major algal symbionts were calculated and compared across almost all genomic dataset samples *Porites* to determine if symbiont proportions differ between geographic location and environment. Sample-specific raw reads from 92 genomic dataset samples were aligned to a concatenated algal transcriptome including four major algal symbiont genera (*Symbiodinium*, *Breviolum*, *Cladocopium*, and *Durusdinium*) with a custom `zoox.pl` script using Bowtie2 (Bayer et al., 2012; Ladner et al., 2012; Manzello et al., 2019). Reads that mapped with a high level of uniqueness (mapping quality ≥ 40) were counted following Manzello et al., (2019) and were used to measure the proportions of symbionts for almost all genomic dataset samples. Algal symbiont proportions were plotted using the same code for ANGSD admixture analysis.

Corresponding Guam's massive *Porites* among other Indo-Pacific *Porites* is important to determine whether Guam's massive *Porites* are comprised of lineages that are found elsewhere throughout the Indo-Pacific or are endemic to Guam. Mitochondrial DNA sequence data for four different primers were generated for a subset of samples from Fouha Bay. A consensus sequence was then generated for each sample by concatenating sample-specific sequences of all four primers. Then, the consensus sequences were included in a separate *Porites* mitochondrial phylogenetic tree containing clades that correspond to a published *Porites* phylogenetic tree (Figure 9; Forsman et al., 2009; Paz-García et al., 2016).

Results

Reads and Loci

From ddRAD sequencing, 238.7 million reads were obtained with an average of 1.2 million reads per sample (SD=1.8 million reads). After the removal of PCR duplicates and quality filtering, 47.4 million reads were retained with an average of 258,785 reads per sample (SD=395,097 reads). Samples with at least 5,000 reads were used for phylogenetic analyses ($n=172$, $\bar{x}=258,785$ reads per sample). Samples with at least 100,000 reads were used for genomic analyses ($n=99$, $\bar{x}=411,227$ reads per sample), respectively. The phylogenetic dataset includes loci present in at least 30% of all samples, with 22,982 genotyped loci and 189,683 SNPs. The genomic dataset includes loci present in at least 80% of all samples, with 12,979 genotyped loci and 31,844 SNPs.

Phylogenetic Analyses

Massive *Porites* Phylogenetics

Phylogenetic analyses revealed six distinct genetic lineages among massive *Porites* on Guam (Figure 2a). All six clades are reciprocally monophyletic and significantly different from one another with perfect node support (100%). The clear distinction of these clades from one another indicates that they most likely represent different species. This would indicate that at least six different species that appear highly similar to *Porites lutea* are present among massive *Porites* on Guam. In addition, one of these clades exhibited significant internal substructure, which might indicate even further differentiation and the presence of additional species among massive *Porites* on Guam. Corallite photographs are included for at least one sample in four out of six clades (Figure 2b). Five of these lineages were assessed in detail for interspecific and intraspecific analyses (Table 1).

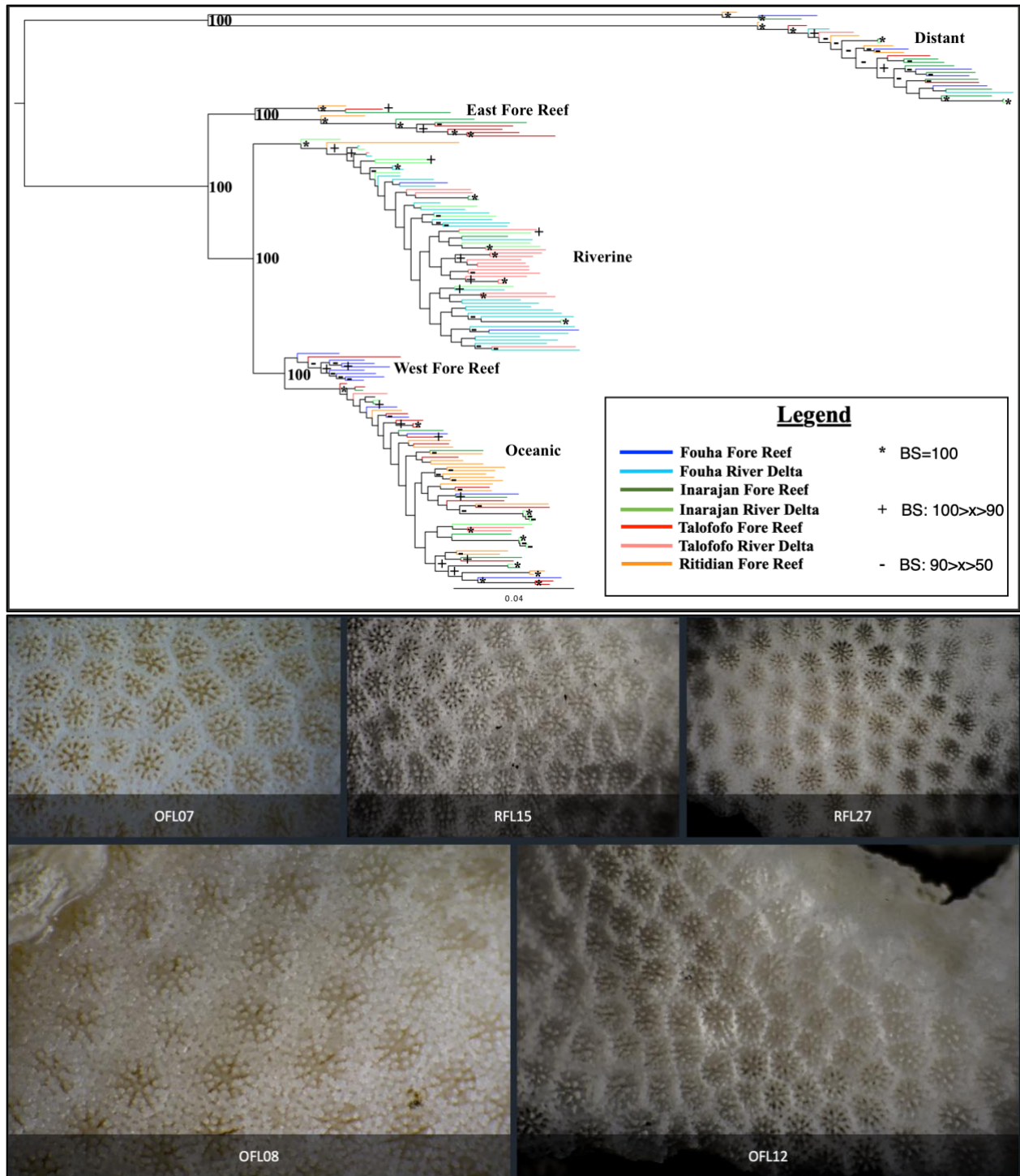


Figure 2: (a) 1000 bootstrap RAxML tree using 189,683 concatenated SNPs with 0 partitions (lnL= -1,698,825). Node colors correspond to the different populations sampled in this study. Bootstrap values are indicated as follows: asterisks indicate full bootstrap support (*=100%), “+” indicate bootstrap values ≥ 90 , “-” indicate bootstrap values $>50- <90$. **(b)** Corallite photos of samples representing 4 out of 6 massive *Porites* lineages. Clade identity is as follows: OFL07 (black outgroup), RFL15 (Riverine), RFL27(Riverine), OFL08 (Distant), OFL12 (Oceanic).

The largest clade (n=64, 37.2% of phylogenetic samples) is referred to as the Riverine clade. Samples in this clade predominantly occur in river delta populations (n=58, 91% of specimen in this clade) and represents 75% of all river delta massive *Porites* in this study. An additional 6 samples in this clade (9%) were collected from fore reef populations (Sup. Material Table 4).

The second-largest clade (n=61, 35.4% of phylogenetic samples) is referred to as the Oceanic clade. Samples in the Oceanic clade predominantly occur in fore reef populations (n=47, 77% of Oceanic clade), representing 49% of fore reef massive *Porites* in this study. An additional 14 samples (23%) are from river delta populations (Sup. Material Table 4).

The third-largest clade is referred to as the Distant clade (n=28, 16.2% of phylogenetic samples, Sup. Material Table 2). Samples in the Distant clade occur in both river delta and fore reef environments, predominantly in Inarajan (43%) and Fouha (20%).

Next, the East Fore Reef clade (n=10, 5.8% of phylogenetic samples) is one of the two smaller clades found exclusively in fore reefs. Samples in this clade occur in Talofofu and Inarajan's fore reefs (both 50%). This clade exhibits significant internal substructure irrespective of geography or environment, indicating that it may consist of two separate species. Samples representing both subclades were included in the PCoA (Fig 3) and NGSAdmix (Fig 4) but pairwise F_{ST} and population genomic summary statistics were calculated using only samples from the main subclade to avoid distorting the aggregate measures.

The West Fore Reef clade (n=9, 5.2% of phylogenetic samples) is the other clade found exclusively in fore reefs. Almost all samples in this clade were found in Fouha's fore reef (89%), with only one sample from Talofofu's fore reef (Sup. Material Table 2).

Finally, the smallest clade, which is colored in black, was represented by one sample each from the fore reef population in Fouha, Inarajan, and Ritidian. Since we only had three samples from this clade, it was not included in subsequent analyses.

Massive *Porites* Environments and Localities

Geography

Most clades were found all around the island but some clades are predominantly represented by samples collected at one geographic location or even one population. For example, almost all of the West fore reef clade's samples are from Fouha's fore reef (8/9 samples; Sup. Material Table 2). In addition, 45% of the Riverine clades samples are from Fouha, while 43% of Distant clade samples are from Inarajan and 50% of East Fore Reef samples are from Talofofu (Sup. Material Table 2).

Environment

Samples were almost evenly collected from fore reef locations (55%) and river deltas (45%). Interestingly, most clades occur either predominantly in river deltas or fore reefs. For example, the Riverine clade is composed of 91% river delta specimens. The Riverine clade also comprises 75% of all river delta samples in the phylogenetic dataset, while all other clades are rarely found in river deltas. Furthermore, the Oceanic clade is composed of 77% fore reef specimens (Sup. Material Table 4). Moreover, the smaller East and West Fore Reef clades were found exclusively in fore reefs. These results indicate that different massive *Porites* clades predominantly occur in different habitats on Guam.

Color

Most clades also exhibit a high fidelity with color phenotype. For example, the West fore reef clade was composed entirely of purple (44%), and brown colonies (56%) (Sup. Material Table

6). However, no exclusive color to clade relationships were found, indicating that color is not a reliable indicator of species identity for massive *Porites* on Guam.

Table 1: Sample count and percentage of samples in genomic analysis for all clades.

Number of samples in phylogenetic and population genomic analyses by clade			
Clade	Phylogenetic	Genomic	% Samples used in genomic analysis
Riverine	64	42	66%
Oceanic	61	28	46%
Distant	28	20	71%
East Fore Reef	10	62	60%
West Fore Reef	9	2	22%
Overall	172	98	53%

Multi-locus genotyping and Clonality

Clonal pairs were either found as single location pairs (SLPs) or multiple location pairs (MLPs), and all triplets were found as single location triplets (Sup. Material Table 7). All SLPs and triplets originate from the same location, regardless of environment, and are documented by the number of pairs or triplets found in each clade with respect to location (Sup. Material Table 7). MLPs are pairs that originate from different locations, also regardless of environment. MLPs are documented by the number of samples from each location belonging to an MLP in each clade (Sup. Material Table 7).

In total, 24 clonal samples were identified and unexpectedly, we found indications for clonality in the four largest clades (Sup. Material Table 7). Most clones were found in the Riverine clade ($n = 10$, 15.6% of Riverine samples), followed by the Oceanic clade with 9 (14.8% of Oceanic samples), the East fore reef clade with 3 (30% of East Fore Reef samples), and the Distant

clade with 2 (7.1% of Distant samples). The remaining number of samples per clade, location and habitat after clonal samples were removed is listed in Table 2.

Most clonal pairs were found within each location, such as the Talofofo river delta samples RTL14 and RTL15. Some pairs, however, were found across populations, such as Ritidian and Inarajan fore reef samples OIL05 and ORL15. Specifically, two multiple location clonal pairs were found between Inarajan and Ritidian, and another one was found between Fouha and Inarajan.

Table 2: Population Genetic Dataset. Per-clade distribution of samples by environment in each geographic location.

	Clade									
	Distant		Oceanic		Riverine		East Fore Reef		West Fore Reef	
Location	River Delta	Fore Reef	River Delta	Fore Reef	River Delta	Fore Reef	River Delta	Fore Reef	River Delta	Fore Reef
Fouha	1	4	0	3	17	1	0	0	0	1
Inarajan	2	8	4	5	8	1	0	2	0	0
Talofofo	1	2	2	4	15	0	0	4	0	1
Ritidian	0	2	0	10	0	0	0	0	0	0
SUM	4	16	6	22	40	2	0	6	0	2

Interspecific Genomic Analyses

A principal coordinate analysis (PCoA) was used to determine the major patterns of genetic differentiation within the genomic dataset (Figure 3). The PCoA shows clear differentiation of samples into the same groups found in the phylogenetic tree. All groups in the PCoA were highly separated from one another, and all samples within each group were tightly clustered together with the exception of the two samples in the West Fore Reef clade. Axis 1 separates the Distant clade from all other clades, especially the East and West Fore Reef clades. Axis 2 separates the Oceanic

and Riverine clades from one another as well as the East and West Fore Reef clades, which are found next to one another.

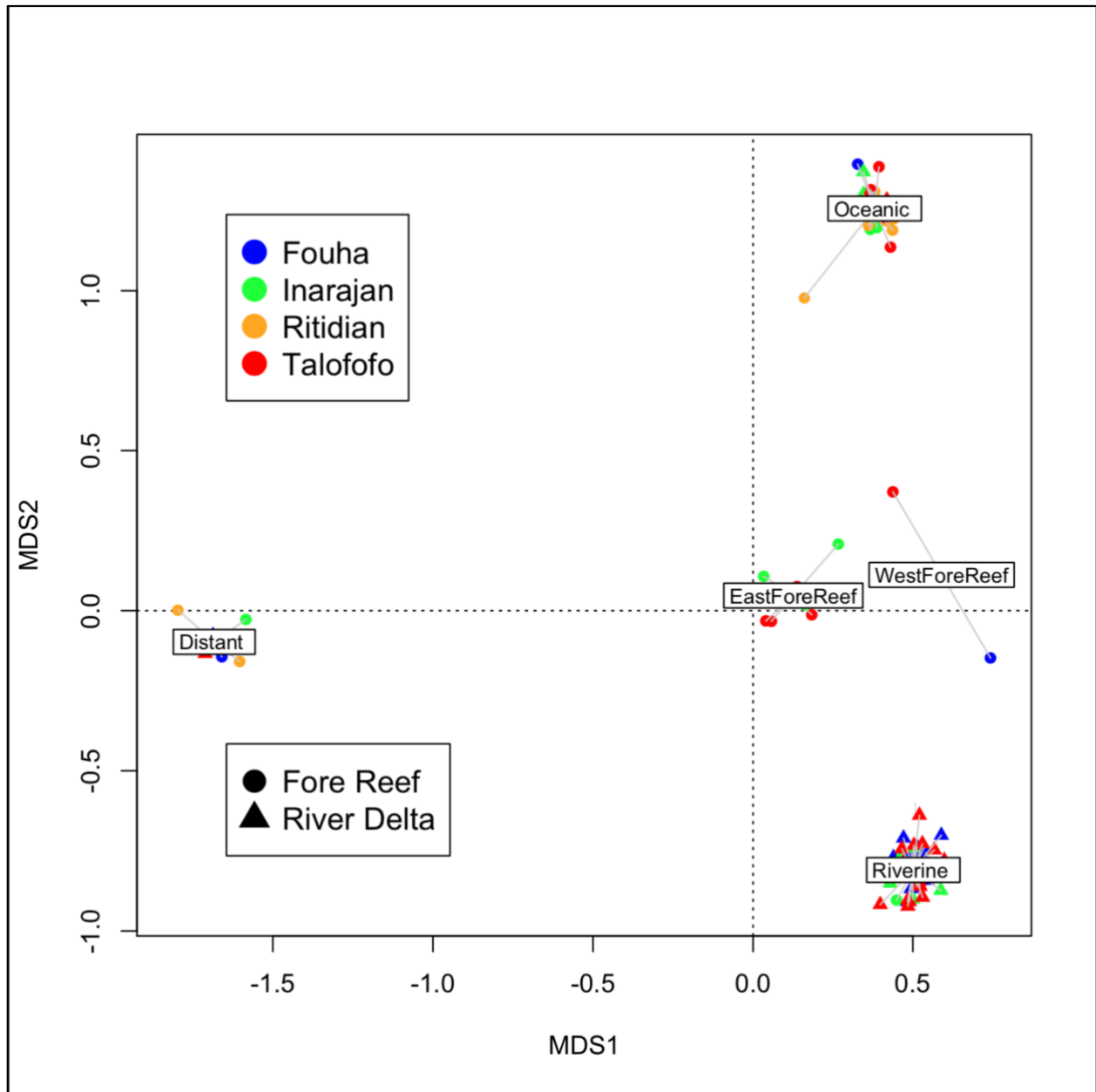


Figure 3: Genomic dataset principal coordinate analysis. Squares indicate samples of fore reef origin, while triangles represent samples of river delta origin.

Admixture plots were generated to infer the most parsimonious number of genetic clusters (K) and identify signature of admixture among clades. Selection of K was implemented via visual

inspection following Manzello et al., (2019) and $K=4$ was identified as the most parsimonious number of genetic clusters. These four genetic clusters corresponded to the Oceanic, Riverine, Distant, and East Fore Reef clades. In general, admixture plots indicated very little gene flow among major clades. However, one sample in the East Fore Reef clade contained ~25% ancestry from the Oceanic clade. Moreover, the ancestry of the two genotypes in the West Fore Reef clade was composed of ~60% Oceanic clade, ~15% Riverine clade, and ~25% East fore reef clade.

Pairwise F_{ST} values among the five clades are high and highly significant, consistent with the finding of these clades being highly divergent at a genome-wide level (Table 3). Pairwise F_{ST} values indicate that the Distant clade is the most distinct of these clades, matching the phylogenetic tree topology, the PCoA and the NGSadmixture result (Figure 2a, 3, 4). The East Fore Reef clade, as well as the Riverine and Oceanic clade appear to be equally differentiated from one another, with only minute differences in all pairwise comparisons. This is different from the pattern on the two dimensional PCoA (Figure 3) but consistent with the phylogenetic tree (Figure 2a). The West Fore Reef clade was removed from this analysis because only two samples from this clade were present in the population genomic dataset.

The genomic dataset AMOVA indicates that almost 61% of all genetic variation is partitioned between clades (Sup. Material Table 9, p -value = 0.001). Genetic diversity is therefore predominantly partitioned between these highly divergent genetic clades. The remaining genetic diversity was mainly partitioned within samples ($F_{IT} = 0.337$) and barely among samples within clades ($F_{IS} = 0.055$) (Sup. Material Table 9). Supporting p -values were not provided in GenoDive for F_{IT} and F_{IS} .

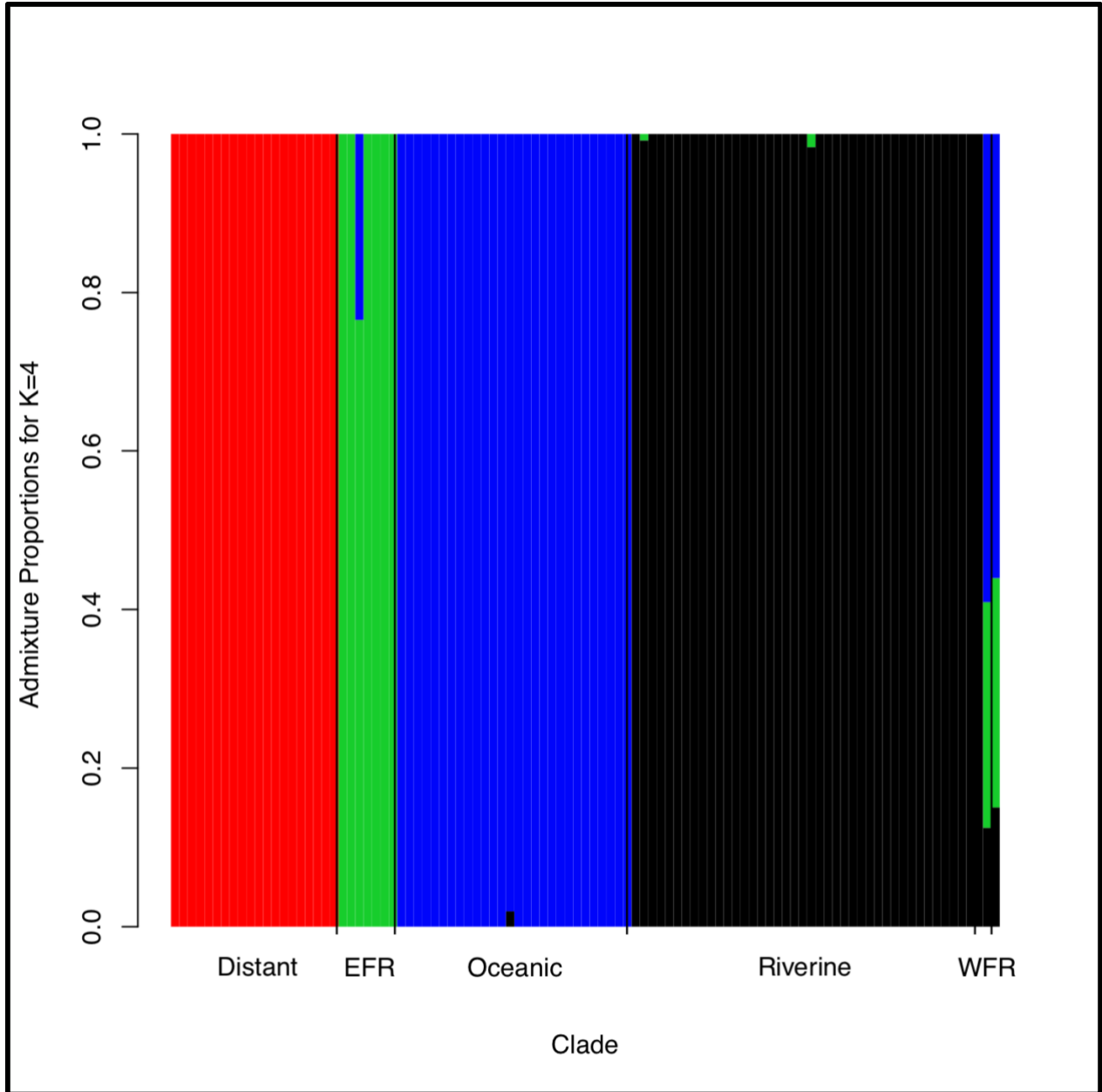


Figure 4: K=4 NGSAdmix plot revealing four discrete major genetic clusters corresponding to the clades in the phylogenetic tree. WFR = West Fore Reef, EFR = East Fore Reef.

Table 3: Pairwise F_{ST} values below diagonal, Bonferroni-corrected p-values above diagonal.

Clade	EFR	Oceanic	Riverine	Distant
EFR		0.010	0.013	0.017
Oceanic	0.249		0.008	0.025
Riverine	0.229	0.185		0.050
Distant	0.397	0.385	0.377	

Population genetic summary statistics (Table 4) indicate that all five clades are fairly similar in these basic population genetic descriptors. The Riverine clade, however, has a slightly higher percentage of polymorphic loci (1.8%), number of private alleles (22,994), nucleotide diversity (0.0025), and observed heterozygosity (0.067) among all clades, but also has the highest level of inbreeding among all clades ($F_{is} = 0.090$) (Table 4). In contrast, the Oceanic clade has a lower observed heterozygosity (0.059), lower nucleotide diversity (0.0020), but lower levels of inbreeding ($F_{is} = 0.053$) compared to the Riverine clade. None of these parameters, however, accounts for the significantly different sample sizes among these clades. For example, the number of private alleles appears to correlate with sample size, therefore, these results should be interpreted with caution.

Table 4: Clade-specific population genetic summary statistics: number of private alleles (Private), observed heterozygosity (H_o), expected heterozygosity (H_e), percent of polymorphic loci (%Poly. loci), inbreeding coefficient (F_{is}), estimate of nucleotide diversity (π).

Clade	Samples	H_o	H_e	%Poly. Loci	F_{is}	π
Riverine	42	0.067	0.081	1.81	0.090	0.0025
Oceanic	28	0.059	0.070	1.08	0.053	0.0020
Distant	20	0.065	0.076	0.96	0.049	0.0022
EFR	6	0.058	0.081	0.64	0.076	0.0020
WFR	2	0.041	0.049	0.29	0.038	0.0016

Intraspecific Genomic Analyses

Clade-specific analyses did not reveal much structure within the Oceanic, Riverine, and Distant clades. For example, the overall NGSAdmix plot (Figure 4), as well as clade specific PCoAs (Figure 5a, 5b & 6) for the Oceanic, Riverine and Distant clades and admixture plots for the Oceanic and Riverine clades (Figure 7a & 7b), all indicate an overall lack of substructure. These results suggest that each clade comprises one discrete genetic entity on Guam with high levels of gene flow between populations and across habitats. Clade-specific AMOVAs indicate that small but significant proportions of genetic diversity are partitioned between populations (Sup. Material Tables 10-12). In the Riverine clade, 1.8% of the genetic diversity was partitioned mainly between river delta samples from all three Southern Guam locations, with the inclusion of a few fore reef samples within the clade (p-value = 0.001, Sup. Material Table 10). In the Oceanic clade, 4.3% of the genetic diversity was partitioned between the four main fore reef populations and additional river delta specimens (p-value = 0.001; Sup. Material Table 11). In the Distant clade, 8.0% of the genetic diversity was partitioned between the four geographic locations that samples in the clade were collected from (p-value = 0.001; Sup. Material Table 12). The remaining genetic diversity in these clades was partitioned both within samples (F_{IT}) and among samples within clades (F_{IS}). All three clades also have similar F_{IS} (Riverine: 0.140, Oceanic: 0.123, Distant: 0.112), indicating mild inbreeding within populations in these clades. F_{IT} values for these clades (Riverine: 0.155, Oceanic: 0.161, Distant: 0.183) indicate moderate levels of differentiation among populations within these clades, despite the lack of internal substructure found within these clades. Three out of six clades in this study correspond to previously recognized Indo-Pacific *Porites*. The black clade corresponds to clade 1 in Figure 9 based on one sample (Forsman et al., (2009). In Forsman et al., (2009), clade 1 contained both branching and mounding *Porites* from Hawai'i, Fiji,

the Galapagos, and Australia. The Distant clade corresponds to clade II in Forsman et al., (2009) based on mtDNA for two samples. This clade consists of *Porites evermanni*, *P. annae*, and *P. sp* from Samoa, Hawai'i and Panama. Based on five Riverine samples, the Riverine clade corresponds to clade V, which consists of both *Porites lutea* and *P. lobata* from American Samoa (Forsman et al., 2009).

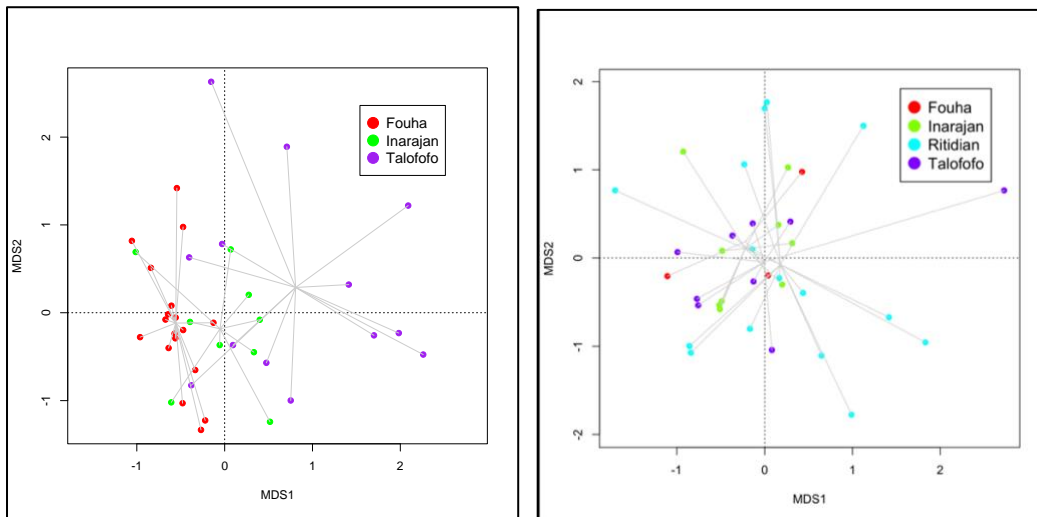


Figure 5: Clade specific PCoAs for a) the Riverine clade and b) the Oceanic clade.

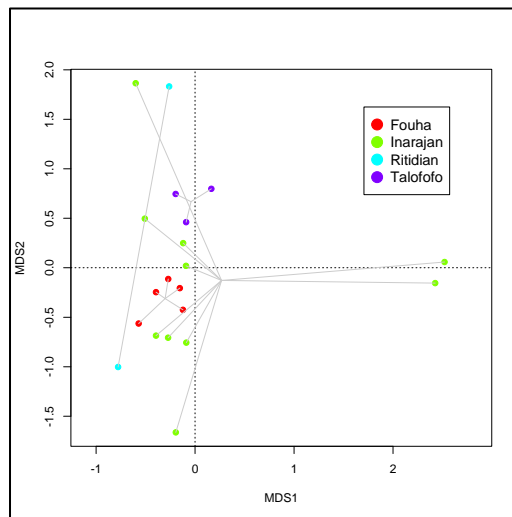
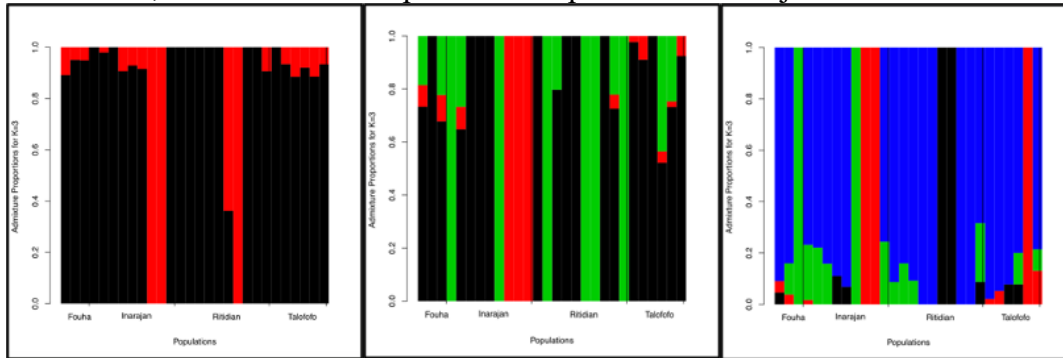
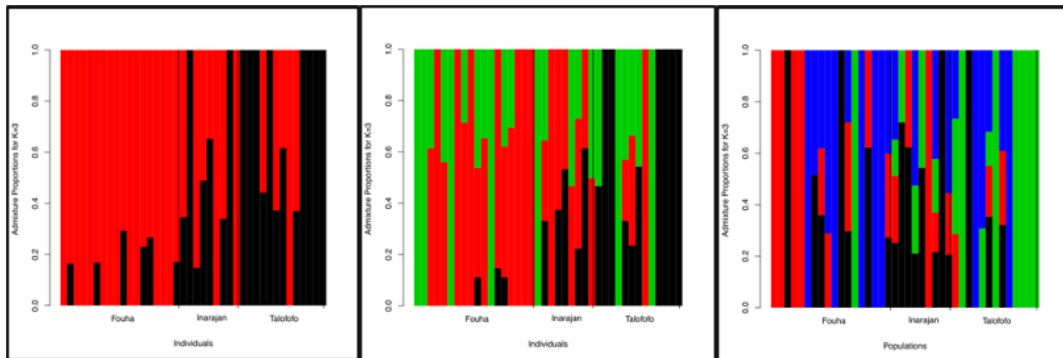


Figure 6: Distant clade population specific PCoA.

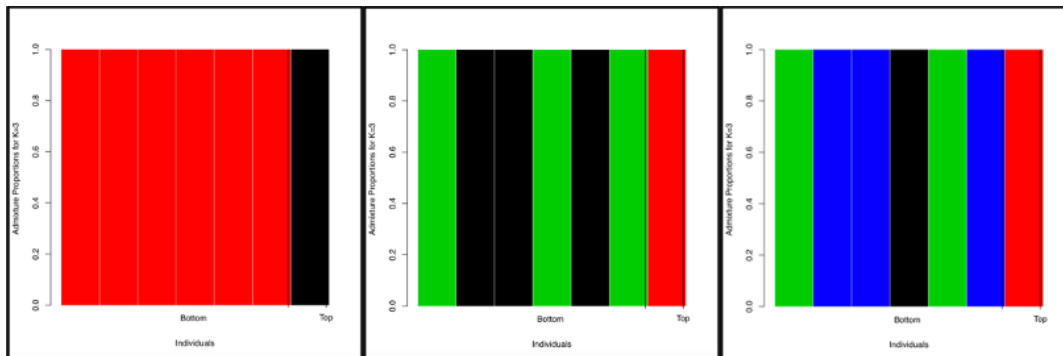
Figures 7a-c: Clade-specific NGSAdmix K=2-4 plots for the Oceanic, Riverine and East Fore Reef clades. Within the East Fore Reef clade, all “Bottom” clade samples are from either Inarajan or Talofoto, while the sole “Top” clade sample is from Inarajan.



7a. Oceanic Clade



7b. Riverine Clade



7c. East Fore Reef Clade

Symbiont Profile Characterization

The dominant symbiont genera were detected for 92 samples across the Oceanic, Riverine, Distant, and East and West Fore Reef clades. In total, 607 reads aligned to the four reference transcriptomes, with 6.7 reads per sample, on average. *Cladocopium* was found to be the dominant

algal symbiont genus in all massive *Porites* specimen assessed, regardless of clade, location and environment (Figure 8). In addition, *Breviolum* was detected in 4 samples and *Durusdinium* was detected in 3 samples while not a single read aligned to *Symbiodinium*. There was no clade-specificity of any symbiont and all three symbionts were detected in multiple clades (Figure 8). Interestingly, 3 out of 4 samples that contained *Breviolum* were found in Riverine samples from river delta environments, while one samples belonged to the Oceanic clade from a fore reef population. *Durusdinium*, on the other hand, was found exclusively in samples from fore reef environments. These results suggest that massive *Porites* predominantly harbor *Cladocopium* regardless of environment and may potentially harbor additional symbionts in different environments. However, the moderate number of symbiont reads per sample provides only limited confidence in these results.

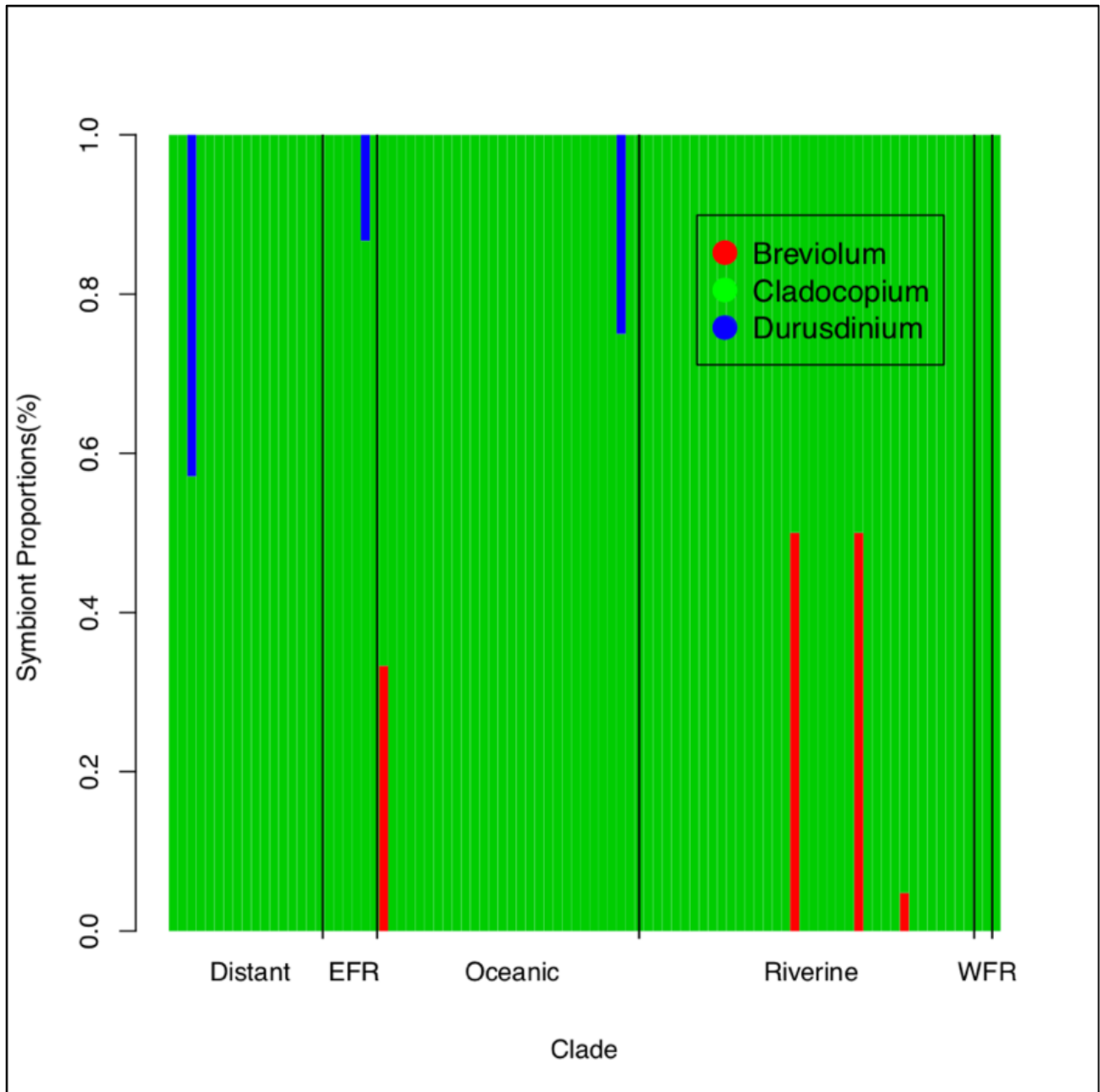


Figure 8: Proportions of four symbiont genera across samples from all clades.

Discussion

Phylogenetic Clade Comparisons

In this study, massive *Porites* from Guam morphologically similar to *Porites lutea* were found to comprise six distinct genetic lineages (Fig. 2). This is a higher number than expected since there are only a few other massive *Porites* on Guam that resemble *Porites lutea*, including *Porites lobata* and *Porites australiensis* (Randall, 2003). All population genomic analyses confirmed five of these lineages (Figures 3, 4; Table 4, S9). Both the overall PCoA and NGSAdmix plot indicate the same genome-wide differentiation of massive *Porites* into the same groups found in the phylogenetic tree (Figures 3, 4). Moreover, pairwise F_{ST} values also indicate high levels of differentiation among clades and an AMOVA revealed that the majority of the total genetic diversity was found among these highly divergent clades (Tables 3, 4). These clades therefore likely represent different *Porites* species, as indicated by the limited admixture found among clades in the genomic dataset NGSAdmix plot (Figure 4).

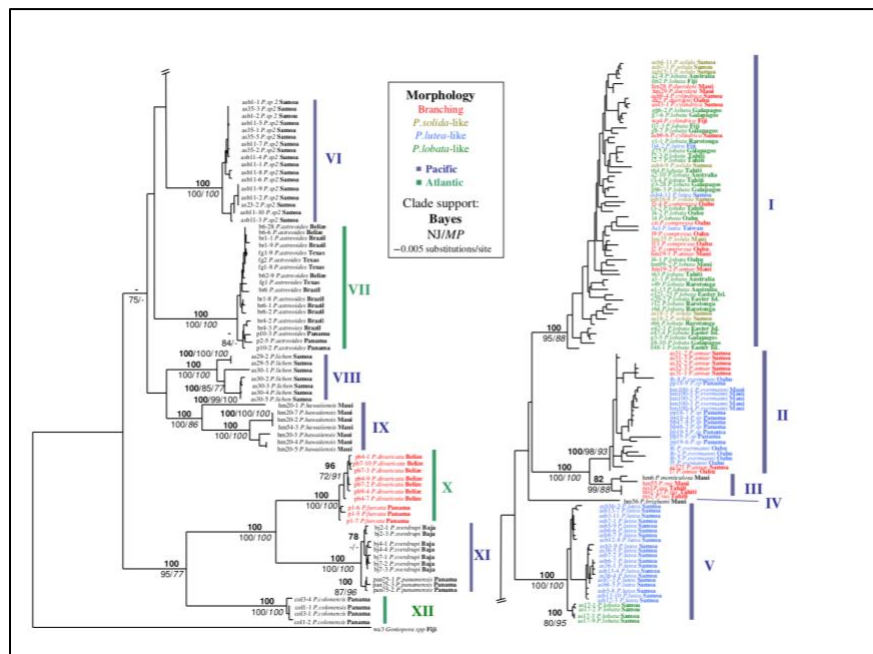


Figure 9: Indo-Pacific and Caribbean *Porites* ITS phylogenetic tree (Forsman et al., 2009).

Morphological convergence is widespread among *Porites*. For example, Forsman et al., (2009) found that massive *Porites* specimens that were morphologically consistent with *Porites lutea* nestled into three distinct phylogenetic clades. In the same study, specimens that were morphologically consistent with *Porites lobata* nestled into two distinct phylogenetic clades. In addition, Boulay et al., (2013) found that massive *Porites* specimens morphologically consistent with *P. lobata* included both *P. lobata* and *P. evermanni*, a morphologically similar yet ecologically distinct species. These cryptic genetic lineages highlight the cryptic genetic diversity among *Porites*. This is not uncommon in other coral genera as well. For example, Bongaerts et al., (2020) unveiled three cryptic, sympatric lineages of *Pachyseris speciosa* throughout the Indo-Pacific who lack morphologically diagnostic characters yet are divergent at a genome-wide level. In another study, Ladner and Palumbi, (2012) identified multiple cryptic species in both the *Acropora cytherea* and *Acropora hyacinthus* species complexes throughout their respective Indo-Pacific distribution. Overlooked, cryptic genetic lineages can hamper proper conservation of foundational reef building taxa (Bongaerts et al., 2020; Boulay et al., 2013). This is because cryptic coral lineages might have more constrained geographic distributions than previously recognized, as well as differing levels of genetic diversity and effective population sizes, which are essential in implementing effective, localized conservation plans. The correspondence of the Oceanic, East Fore Reef and West Fore Reef clades to recognized Indo-Pacific *Porites* is still ongoing and will be included into future versions of this manuscript.

Admixture plots indicate virtually no gene flow between the major lineages of massive *Porites* on Guam. There is, however, the possibility of gene flow among the smaller lineages. For instance, one sample in the EFR clade shows admixture from the Oceanic clade and the WFR clade shows admixture from three other clades (East Fore Reef, Oceanic, and Rivserine). The observed

25% admixture from the Oceanic clade in one EFR sample corresponds to the proportion expected for an F2 hybrid. However, no signs of Oceanic admixture were detected in the other 6 EFR samples included in this analysis (Figure 4). The admixture in the two WFR samples is more complicated and might indicate a complex hybrid origin of this clade. Hybridization has been previously reported among Indo-Pacific *Porites*. For example, Forsman et al., (2017) failed to resolve morphologically distinct *Porites lobata* and *Porites compressa* in Hawaii as distinct species, suggesting that these morphospecies might hybridize extensively. In another study, Hellberg et al., (2016) revealed introgression from *Porites evermanni* into *Porites lobata* in the eastern Pacific, contrary to the reported lack of gene flow between these species in both Hawaii and American Samoa. This suggests that certain lineages of massive *Porites* on Guam undergo hybridization. Specific analyses of interspecific introgression among clades are ongoing and will be included into future versions of this manuscript.

Another interesting finding is the presence of clones in four clades: the Riverine, Oceanic, Distant, and East Fore Reef clades (Sup. Material Table 7). Clonality has occasionally been mentioned for massive *Porites* before. For example, (Boulay et al., 2013) reported that *Porites evermanni* reproduces asexually via fragmentation due to triggerfish predation in the Eastern Pacific. Moreover, Brown et al., (2020) found a *Porites* lineage confined to Honolulu Harbor that reproduces by generating presumably clonal larvae, with colonies of various sizes found to fuse together. These results suggest that clonality in massive *Porites* can be driven by a variety of different biotic or abiotic factors. It is still unclear, however, as to how the four lineages of massive *Porites* in this study generate clones.

Another notable finding of this study is that the Riverine *Porites* predominantly occupy a habitat where other *Porites* species are much less common (Sup. Material Table 4). This indicates

that this lineage is adapted to this particular habitat. The extent of differentiation and lack of gene flow between the Riverine clade and all other clades (Figure 3, 4), as well as the overwhelming presence of Riverine clade samples to river deltas, all suggest that the Riverine clade may have adapted to these marginal turbid-zone habitats. Specific analyses for signature of selection are ongoing and will be included into subsequent versions of this manuscript.

Genetic differentiation among congeneric coral taxa due to environmental differences have been previously reported for *Porites*. For example, environmental differences were found to drive coral host population structure between nearshore and offshore *P. astreoides* in the Florida Keys, despite a lack of genetic structure between *P. astreoides* symbionts in these sites (Kenkel et al., 2013). Nearshore *P. astreoides* experiencing considerable temperature variation exhibited lower levels of bleaching compared to offshore *P. astreoides* that were buffered by both the Hawk Channel and Gulf Stream. A similar pattern of environmental differentiation was found in *Porites* in Hawaii. Brown et al., (2020) found a population of bleaching resistant brooding *Porites* that live in a highly polluted and sedimented habitat within Honolulu Harbor. These "Harbor *Porites*" are genetically distinct but similar to the broadcast spawning *Porites lobata* species complex (ITS: 99.4%; histone: 99.9%). In another study, Tisthammer et al., (2020) found nearshore and offshore populations of *P. lobata* in both Wahikuli and Oahu to be genetically distinct. Interestingly, pairwise genetic differentiation between Oahu's sites were nearly identical to GenoDive pairwise F_{ST} values between the Riverine and Oceanic clades ($F_{ST} = 0.19$ and 0.185 , respectively). These collective findings suggest that massive *Porites* found in different habitats may frequently constitute discrete genetic entities.

A general lack of substructure was found among populations within the Riverine, Oceanic, and Distant clades, the three most numerous lineages of massive *Porites* on Guam (Figures 5, 6,

7, Supplementary Material Tables 10, 11, & 12). A similar lack of population structure around Guam have been reported in other studies. For example, Tusso et al., (2016) found a lack of population structure among crown-of-thorns seastar (*Acanthaster planci*) populations on Guam. On the other hand, Boulay et al., (2014) found extensive population structure of *Acropora pulchra* between Guam and nearby Cocos Lagoon due to extensive asexual fragmentation and oceanographic currents acting as a barrier for gene flow between sites. The lack of internal substructure in the Oceanic, Riverine, and Distant clades is most likely due to Guam's small size and the fact that massive *Porites* are generally broadcast spawners (Morton & Perry, 1999; Randall, 2003).

Population genetic summary statistics indicate that all five clades are fairly similar in these basic population genetic descriptors (Table 4). For example, nucleotide diversity is significantly lower across clades in this study than nucleotide diversity reported for Hawai'ian *Porites compressa* in Locatelli & Drew (2019) (\bar{x} [Locatelli]=0.21; \bar{x} [present study]=0.0021), who also employed a ddRAD approach to generate their genetic data. This is likely due to the fact that there was a lack of gene flow between the lineages found in this study, whereas *Porites compressa* has been found to hybridize extensively with *Porites lobata*. *Porites compressa* therefore likely has a higher effective population size than the lineages in this study, leading to higher nucleotide diversity in the species. Inbreeding coefficients are also consistently low across clades, which is expected for broadcast spawners, with similar findings in Locatelli & Drew, (2019) (\bar{x} [Locatelli]=0.0684; \bar{x} [present study]=0.0612). Slight heterozygote deficit is also a common feature among marine populations, as was the case in this study (Ayre & Hughes, 2000).

Among all clades, however, the Riverine clade, which is the largest of all clades, was found to be slightly but consistently more genetically diverse than others (Table 4), likely due to sample

size bias in STACKS. It had the highest nucleotide diversity, % polymorphic loci, expected and observed heterozygosity and private alleles than all other clades. In contrast, the Oceanic clade had much less inbreeding than the Riverine clade. This is likely due to the discontinuous presence of these geographically proximal river delta habitats from one another, whereas the fore reef populations exhibit high levels of gene flow on an island-wide scale. These results should be interpreted with caution, however, since sample size bias was not accounted for in this analysis.

Symbionts

Cladocopium was found to be the dominant symbiont clade among all massive *Porites* on Guam, irrespective of clade identity, location or habitat. *Cladocopium* is the most common coral symbiont throughout the Caribbean and Indo-Pacific (LaJeunesse et al., 2018). Among *Porites* corals, *Cladocopium* C15 was found to be the major algal symbiont among 15 *Porites lutea* populations in Singapore and Eastern and Western Peninsular Malaysia (Tan et al., 2020). *Cladocopium* was also found to be the dominant algal symbiont among Hawaiian corals within the *Porites lobata* species complex (Forsman et al., 2020).

Durusdinium and *Breviolum* were found as secondary symbionts in a subset of massive *Porites* across clades. Their presence among habitats was somewhat skewed, indicating the possibility that they are more common in fore reefs and river deltas, respectively. Specifically, *Durusdinium* was found exclusively in fore reef specimens, while *Breviolum* was found almost exclusively in river delta specimens. *Durusdinium* species have been found to be tolerant against thermal stress (Brian et al., 2019; Chen et al., 2020; Gong et al., 2019; Tan et al., 2020). The high fidelity of *Durusdinium* to fore reef specimens indicates that fore reef massive *Porites* might host symbionts that have higher thermotolerance to mitigate the effects of high irradiance and sea surface temperature on these corals during bleaching events. On the other hand, *Breviolum* has

been found to respond positively to high-nitrogen environments (Bayliss et al., 2019). Rivers deposit high volumes of sediment and particulate matter into nearby deltas, with nitrogen being one of many nutrients found in high concentrations in these areas (Jarvie et al., 2018; Meybeck, 1982; Xia, et al., 2018). The high fidelity of *Breviolum* to river delta specimens indicates that river delta massive *Porites* might host symbionts that have a higher tolerance for eutrophication.

Conservation

This study provides insight into the population dynamics of ecologically significant massive *Porites*, both on an island-wide scale and between two starkly different habitats. This is critical for conservation management since *Porites* has been identified as resilient to bleaching and increased sea surface temperature, contrary to other vulnerable coral genera, such as staghorn *Acropora* (Brown et al., 2020; Jokiel & Brown, 2004; Raymundo et al., 2019; Sully & van Woesik, 2020). Monitoring the status of massive *Porites* is critical, especially for the Riverine clade, who predominantly occupies marginal, turbid-zone river delta habitats that most other corals cannot survive in. Marginal reef corals have been found to possess more stress resilient traits and are likely adapted to living in sub-optimal conditions inherent to river deltas (de Oliveira Soares, 2020; Tisthammer et al., 2020). These corals, however, are threatened by land use change that includes, but is not limited to dredging, deforestation, and erosion (de Oliveira Soares, 2020). Marginal reef degradation due to land use change is a significant issue on Guam, where Wolanski et al., (2004) found that terrigenous mud was responsible for both high levels of mortality and an inability of corals to recover in Fouha Bay after land clearing and road construction that led to sediment-laden runoff between 1988-1990. In some areas, perpetual land use change and anthropogenic activity has resulted in a more extensive impact of river runoff on coral reefs. For example, Wooldridge et al., (2006) found that the impact of Post-European settlement nutrient enrichment from runoff in

the Great Barrier Reef ranges from between 20-30 km offshore, as compared to pre-European settlement nutrient enrichment that was constrained to only 1-2 km offshore. Modeling the future population dynamics of massive *Porites* on Guam across different environments is therefore critical to preserve local massive *Porites* biodiversity.

Conclusions

In this study, I unveiled multiple genetic clades of massive *Porites* on Guam exhibiting genome-wide divergence utilizing a ddRAD, next-generation sequencing approach. Some clades were found to predominantly occur in either turbid river deltas or oceanic fore reefs, indicating that certain massive *Porites* lineages on Guam may be predisposed to occupying specific environments. A lack of substructure was found within the Oceanic and Riverine clades. Samples in the East and West Fore Reef clade showed signs of interspecific admixture. *Cladocopium* was found to be the dominant algal symbiont among Guam's massive *Porites* lineages, however, massive *Porites* occupying river deltas and fore reefs may harbor other symbionts adapted to living in these different environments. Conservation of these massive *Porites*, especially those found in marginal habitats, is imperative in preserving the diversity of this foundational reef-building coral in the face of ongoing climate change.

Literature Cited

1. Ayre, D. J., & Hughes, T. P. (2000). Genotypic diversity and gene flow in brooding and spawning corals along the great barrier reef, Australia. *Evolution*, 54(5), 1590–1605.
2. Barfield S., Davies S., Matz M.V. (2020). Co-recruitment of relatives in a broadcast-spawning coral (*Acropora hyacinthus*) facilitates emergence of an inbred, genetically distinct group within a panmictic population. *BioRxiv*.
3. Bayer, T., Aranda, M., Sunagawa, S., Yum, L. K., DeSalvo, M. K., Lindquist, E., Coffroth, M. A., Voolstra, C. R., & Medina, M. (2012). Symbiodinium transcriptomes: Genome insights into the dinoflagellate symbionts of reef-building corals. *PLoS ONE*, 7(4).
4. Bayliss, S. L. J., Scott, Z. R., Coffroth, M. A., & terHorst, C. P. (2019). Genetic variation in *Breviolum antillogorgium*, a coral reef symbiont, in response to temperature and nutrients. *Ecology and Evolution*, 9(5), 2803–2813.
5. Bongaerts, P., Cooke, I., Ying, H., Wels, D., S, H. Den, Brunner, C., Dove, S., Englebert, N., & Eyal, G. (2020). Cryptic diversity masks ecologically distinct coral species on tropical reefs. *BioRxiv*, 20, 34.
6. Bongaerts, P., Riginos, C., Brunner, R., Englebert, N., Smith, S. R., & Hoegh-Guldberg, O. (2017). Deep reefs are not universal refuges: Reseeding potential varies among coral species. *Science Advances*, 3(2).
7. Boulay, J. N., D. Burdick, A. Halford, J. McIlwain, and I. B. B. (2014). Genetic connectivity and spatial clonal structure in a dominant staghorn coral on reefs around Guam. *Penn State Library, December*, 96–135.
8. Boulay, J. N., Hellberg, M. E., Cortés, J., & Baums, I. B. (2013). Unrecognized coral species diversity masks differences in functional ecology. *Proceedings of the Royal Society B: Biological Sciences*, 281(1776), 20131580.
9. Brian, J.I., Davy, S.K. and Wilkinson, S. P. (2019). Elevated Symbiodiniaceae richness at Atauro Island (Timor-Leste): a highly biodiverse reef system. *Coral Reefs*, 38(1), 123–136.
10. Brown, N. P., Forsman, Z. H., Tisthammer, K. T., & Richmond, R. H. (2020). A resilient brooding coral in the broadcast spawning *Porites lobata* species complex: a new endemic, introduced species, mutant, or new adaptive potential? *Coral Reefs*, 39(3), 809–818.
11. Bruno, J. F., & Selig, E. R. (2007). Regional decline of coral cover in the Indo-Pacific: Timing, extent, and subregional comparisons. *PLoS ONE*, 2(8).
12. Catchen, J. M. (2013). Stacks: an analysis tool set for population genomics. *Molecular Ecology*, 22(11), 3124–3140.
13. Catchen, J. M., Amores, A., Hohenlohe, P., Cresko, W., & Postlethwait, J. H. (2011). *Stacks : Building and Genotyping Loci De Novo From Short-Read Sequences. G3: Genes/Genomes/Genetics*, 1(3), 171–182.

14. Chen, B., Yu, K., Qin, Z., Liang, J., Wang, G., Huang, X., Wu, Q. and Jiang, L. (2020). Dispersal, genetic variation, and symbiont interaction network of heat-tolerant endosymbiont *Durusdinium trenchii*: Insights into the adaptive potential of coral to climate change. *Science of the Total Environment*.
15. Combosch, D. J., Lemer, S., Ward, P. D., Landman, N. H., & Giribet, G. (2017). Genomic signatures of evolution in *Nautilus*—An endangered living fossil. *Molecular Ecology*, 26(21), 5923–5938.
16. de Oliveira Soares, M. (2020). Marginal reef paradox: A possible refuge from environmental changes? *Ocean & Coastal Management*, 185.
17. Doney, S. C., Ruckelshaus, M., Emmett Duffy, J., Barry, J. P., Chan, F., English, C. A., Galindo, H. M., Grebmeier, J. M., Hollowed, A. B., Knowlton, N., Polovina, J., Rabalais, N. N., Sydeman, W. J., & Talley, L. D. (2012). Climate Change Impacts on Marine Ecosystems. *Annual Review of Marine Science*, 4(1), 11–37.
18. Forsman, Z. H., Knapp, I. S. S., Tisthammer, K., Eaton, D. A. R., Belcaid, M., & Toonen, R. J. (2017). Coral hybridization or phenotypic variation? Genomic data reveal gene flow between *Porites lobata* and *P. Compressa*. *Molecular Phylogenetics and Evolution*, 111(March), 132–148.
19. Forsman, Z., Ritson-Williams, R., Tisthammer, K. H., Knapp, I. S. S., & Toonen, R. J. (2020). Host-symbiont coevolution, cryptic structure, and bleaching susceptibility, in a coral species complex (Scleractinia; Poritidae). *Scientific Reports*, 10(1), 1–12.
20. Forsman, Z., Wellington, G. M., Fox, G. E., & Toonen, R. J. (2015). Clues to unraveling the coral species problem: distinguishing species from geographic variation in *Porites* across the Pacific with molecular markers and microskeletal traits. *PeerJ*, 3, e751.
21. Forsman, Z., Barshis, D. J., Hunter, C. L., & Toonen, R. J. (2009). Shape-shifting corals: Molecular markers show morphology is evolutionarily plastic in *Porites*. *BMC Evolutionary Biology*, 9(1), 1–9.
22. Frade, P. R., Bongaerts, P., Englebert, N., Rogers, A., Gonzalez-rivero, M., & Hoegh-guldberg, O. (2018). Deep reefs of the Great Barrier Reef offer limited thermal refuge during mass coral bleaching. *Nature Communications*, 1–8.
23. Gardner, T.A., Côté, I.M., Gill, J.A., Grant, A. and Watkinson, A. R. (2005). Hurricanes and Caribbean coral reefs: impacts, recovery patterns, and role in long-term decline. *Ecology*, 86(1), 174–184.
24. Gong, S., Xu, L., Yu, K., Zhang, F. and Li, Z. (2019). Differences in Symbiodiniaceae communities and photosynthesis following thermal bleaching of massive corals in the northern part of the South China Sea. *Marine Pollution Bulletin*, 144, 196–204.
25. Goreau, T., Mcclanahan, T., Hayes, R., Strong, A., Bleaching, C., & Surface, S. (2016). *Society for Conservation Biology Conservation of Coral Reefs after the 1998 Global Bleaching Event Published by : Wiley for Society for Conservation Biology Linked references are available on JSTOR for this article : Issues in International Conservation C. 14(1), 5–15*
26. Grottoli, A. G., Rodrigues, L. J., & Palardy, J. E. (2006). Heterotrophic plasticity and resilience in bleached corals. *Nature*, 440(7088), 1186–1189.

27. Guest, J. R., Tun, K., Low, J., Vergés, A., Marzinelli, E. M., Campbell, A. H., Bauman, A. G., Feary, D. A., Chou, L. M., & Steinberg, P. D. (2016). 27 years of benthic and coral community dynamics on turbid, highly urbanised reefs off Singapore. *Scientific Reports*, 6(November), 1–10.
28. Hellberg, M. E., Prada, C., Tan, M. H., Forsman, Z. H., & Baums, I. B. (2016). Getting a grip at the edge: recolonization and introgression in eastern Pacific Porites corals. *Journal of Biogeography*, 43(11), 2147–2159.
29. Hodgson, G. (1990). Tetracycline reduces sedimentation damage to corals. *Marine Biology*, 104(3), 493–496.
30. Hoegh-Guldberg, O., Mumby, P. J., Hooten, A. J., Steneck, R. S., Greenfield, P., Gomez, E., Harvell, C. D., Sale, P. F., Edwards, A. J., Caldeira, K., Knowlton, N., Eakin, C. M., Iglesias-Prieto, R., Muthiga, N., Bradbury, R. H., Dubi, A., & Hatziolos, M. E. (2007). Coral reefs under rapid climate change and ocean acidification. *Science (New York, N.Y.)*, 318(5857), 1737–1742.
31. Hoogenboom, M. O., Frank, G. E., Chase, T. J., Jurriaans, S., Álvarez-Noriega, M., Peterson, K., Critchell, K., Berry, K. L. E., Nicolet, K. J., Ramsby, B., & Paley, A. S. (2017). Environmental drivers of variation in bleaching severity of Acropora species during an extreme thermal anomaly. *Frontiers in Marine Science*, 4(NOV), 1–16.
32. Horton, T., Kroh, A., Ahyong, S., Bailly, N., Boyko, C. B., Brandão, S. N., Gofas, S., Hooper, J. N. A., Hernandez, F., Holovachov, O., Mees, J., Molodtsova, T. N., Paulay, G., Decock, W., Dekeyzer, S., Poffyn, G., Vandepitte, L., Vanhoorne, B., Adlard, R., ... Zhao, Z. (2020). *World Register of Marine Species (WoRMS)*. WoRMS Editorial Board.
33. Hughes, A. D., & Grottoli, A. G. (2013). Heterotrophic compensation: A possible mechanism for resilience of coral reefs to global warming or a sign of prolonged stress? *PLoS ONE*, 8(11), 1–10.
34. Hughes, T. P., Rodrigues, M. J., Bellwood, D. R., Ceccarelli, D., Hoegh-Guldberg, O., McCook, L., Moltschaniwskyj, N., Pratchett, M. S., Steneck, R. S., & Willis, B. (2007). Phase Shifts, Herbivory, and the Resilience of Coral Reefs to Climate Change. *Current Biology*, 17(4), 360–365.
35. Humanes, A., Ricardo, G. F., Willis, B. L., Fabricius, K. E., & Negri, A. P. (2017). Cumulative effects of suspended sediments, organic nutrients and temperature stress on early life history stages of the coral *Acropora tenuis*. *Scientific Reports*, 7(March), 1–11.
36. Ihaka, R., & Gentleman, R. (1996). R: A language for data analysis. In *Journal of Computational and Graphical Statistics* (Vol. 5, pp. 299–314).
37. Jarvie, H. P., Smith, D. R., Norton, L. R., Edwards, F. K., Bowes, M. J., King, S. M., Scarlett, P., Davies, S., Dils, R. M., & Bachiller-Jareno, N. (2018). Phosphorus and nitrogen limitation and impairment of headwater streams relative to rivers in Great Britain: A national perspective on eutrophication. *Science of the Total Environment*, 621, 849–862.
38. Jokiel, P. L., & Brown, E. K. (2004). Global warming, regional trends and inshore environmental conditions influence coral bleaching in Hawaii. *Global Change Biology*, 10(10), 1627–1641.

39. Kenkel, C. D., Goodbody-Gringley, G., Caillaud, D., Davies, S. W., Bartels, E., & Matz, M. V. (2013). Evidence for a host role in thermotolerance divergence between populations of the mustard hill coral (*Porites astreoides*) from different reef environments. *Molecular Ecology*, 22(16), 4335–4348.
40. Korneliusen, T. S., Albrechtsen, A., & Nielsen, R. (2014). ANGSD: Analysis of Next Generation Sequencing Data. *BMC Bioinformatics*, 15(1), 1–13.
41. Ladner, J.T. and Palumbi, S. R. (2012). Extensive sympatry, cryptic diversity and introgression throughout the geographic distribution of two coral species complexes. *Molecular Ecology*, 21(9), 63–132.
42. Ladner, J. T., Barshis, D. J., & Palumbi, S. R. (2012). Protein evolution in two co-occurring types of Symbiodinium: An exploration into the genetic basis of thermal tolerance in Symbiodinium clade D. *BMC Evolutionary Biology*, 12(1).
43. LaJeunesse, T. C., Parkinson, J. E., Gabrielson, P. W., Jeong, H. J., Reimer, J. D., Voolstra, C. R., & Santos, S. R. (2018). Systematic Revision of Symbiodiniaceae Highlights the Antiquity and Diversity of Coral Endosymbionts. *Current Biology*, 28(16), 2570-2580.e6.
44. Langmead, B., & Salzberg, S. L. (2012). Fast gapped-read alignment with Bowtie 2. *Nature Methods*, 9(4), 357–359.
45. Locatelli, N., & Drew, J. (2019). Population structure and clonal prevalence of scleractinian corals (*Montipora capitata* and *Porites compressa*) in Kaneohe Bay, Oahu. *BioRxiv*, 1–31.
46. Loiola, M., Cruz, I.C., Lisboa, D.S., Mariano-Neto, E., Leão, Z.M., Oliveira, M.D. and Kikuchi, R. K. (2019). Structure of marginal coral reef assemblages under different turbidity regime. *Marine Environmental Research*, 147, 138–148.
47. Manzello, D. P., Matz, M. V., Enochs, I. C., Valentino, L., Carlton, R. D., Kolodziej, G., Serrano, X., Towle, E. K., & Jankulak, M. (2019). Role of host genetics and heat-tolerant algal symbionts in sustaining populations of the endangered coral *Orbicella faveolata* in the Florida Keys with ocean warming. *Global Change Biology*, 25(3), 1016–1031.
48. Martin, M. (2011). Cutadapt removes adapter sequences from high-throughput sequencing reads. *EMBnet*, 17(1), 10–12.
49. Meybeck, M. (1982). Carbon, nitrogen, and phosphorus transport by world rivers. In *American Journal of Science* (Vol. 282, Issue 4, pp. 401–450).
50. Miller, M.A., Pfeiffer, W. and Schwartz, T. (2010). Creating the CIPRES Science Gateway for inference of large phylogenetic trees. *2010 Gateway Computing Environments Workshop*, 1–8.
51. Morgan, K. M., Perry, C. T., Johnson, J. A., & Smithers, S. G. (2017). Nearshore Turbid-Zone Corals Exhibit High Bleaching Tolerance on the Great Barrier Reef Following the 2016 Ocean Warming Event. *Frontiers in Marine Science*, 4(July), 1–13.
52. Morton, J. M., & Perry, G. (1999). Regeneration Rates Of The Woody Vegetation Of Guam's Northwest Field Following Major Disturbance: Land Use Patterns, Feral Ungulates, And Cascading Effects Of The Brown Treesnake. *Micronesica*, 32(1), 125–142.

53. Myers, R. L., & Raymundo, L. J. (2009). Coral disease in Micronesian reefs: A link between disease prevalence and host abundance. *Diseases of Aquatic Organisms*, 87(1–2), 97–104.
54. Paz-García, D. A., Galván-Tirado, C., Alvarado, J. J., Cortés, J., García-De-León, F. J., Hellberg, M. E., & Balart, E. F. (2016). Variation in the whole mitogenome of reef-building *Porites* corals. *Conservation Genetics Resources*, 8(2), 123–127.
55. Peterson, B. K., Weber, J. N., Kay, E. H., Fisher, H. S., & Hoekstra, H. E. (2012). Double digest RADseq: An inexpensive method for de novo SNP discovery and genotyping in model and non-model species. *PLoS ONE*, 7(5).
56. Pollock, F. J., Lamb, J. B., Field, S. N., Heron, S. F., Schaffelke, B., Shedrawi, G., Bourne, D. G., & Willis, B. L. (2014). Sediment and turbidity associated with offshore dredging increase coral disease prevalence on nearby reefs. *PLoS ONE*, 9(7).
57. Porter, S. N., & Schleyer, M. H. (2017). Long-term dynamics of a high-latitude coral reef community at Sodwana Bay, South Africa. *Coral Reefs*, 36(2), 369–382.
58. Prada, C., De Biasse, M. B., Neigel, J. E., Yednock, B., Stake, J. L., Forsman, Z. H., Baums, I. B., & Hellberg, M. E. (2014). Genetic species delineation among branching Caribbean *Porites* corals. *Coral Reefs*, 33(4), 1019–1030.
59. Randall, R. H. (2003). An annotated checklist of hydrozoan and scleractinian corals collected from Guam and other Mariana Islands. *Micronesica*, 35–36, 121–137.
60. Raymundo, L. J., Burdick, D., Hoot, W. C., Miller, R. M., Brown, V., Reynolds, T., Gault, J., Idechong, J., Fifer, J., & Williams, A. (2019). Successive bleaching events cause mass coral mortality in Guam, Micronesia. *Coral Reefs*, 38(4), 677–700.
61. Sully, S., & van Woesik, R. (2020). Turbid reefs moderate coral bleaching under climate-related temperature stress. *Global Change Biology*, 26(3), 1367–1373.
62. Tan, Y. T. R., Wainwright, B. J., Afiq-Rosli, L., Ip, Y. C. A., Lee, J. N., Nguyen, N. T. H., Pointing, S. B., & Huang, D. (2020). Endosymbiont diversity and community structure in *Porites lutea* from Southeast Asia are driven by a suite of environmental variables. *Symbiosis*, 80(3), 269–277.
63. Teixeira, C.D., Leitão, R.L., Ribeiro, F.V., Moraes, F.C., Neves, L.M., Bastos, A.C., Pereira-Filho, G.H., Kampel, M., Salomon, P.S., Sá, J.A. and Falsarella, L. N. (2019). Sustained mass coral bleaching (2016–2017) in Brazilian turbid-zone reefs: taxonomic, cross-shelf and habitat-related trends. *Coral Reefs*, 38(4), 801–813.
64. Terraneo, T. I., Benzoni, F., Baird, A. H., Arrigoni, R., & Berumen, M. L. (2019). Morphology and molecules reveal two new species of *Porites* (Scleractinia, Poritidae) from the Red Sea and the Gulf of Aden. *Systematics and Biodiversity*, 17(5), 491–508.
65. Tisthammer, K.H., Timmins-Schiffman, E., Seneca, F.O., Nunn, B.L. and Richmond, R. H. (2020). Surviving in high stress environments: Physiological and molecular responses of lobe coral indicate nearshore adaptations to anthropogenic stressors. *BioRxiv*.
66. Tisthammer, K. H., Forsman, Z. H., Toonen, R. J., & Richmond, R. H. (2020). Genetic structure is stronger across human-impacted habitats than among islands in the coral *Porites lobata*. *PeerJ*, 2020(2), 1–24.

67. Tusso, S., Morcinek, K., Vogler, C., Schupp, P. J., Caballes, C. F., Vargas, S., & Wörheide, G. (2016). Genetic structure of the crown-of-thorns seastar in the Pacific Ocean, with focus on Guam. *PeerJ*, 2016(5), 1–22.
68. Van Woesik, R., Houk, P., Isechal, A. L., Idechong, J. W., Victor, S., & Golbuu, Y. (2012). Climate-change refugia in the sheltered bays of Palau: Analogs of future reefs. *Ecology and Evolution*, 2(10), 2474–2484.
69. Voolstra, C. R., Miller, D. J., Ragan, M. A., Hoffmann, A. A., Hoegh-Guldberg, O., Bourne, D. G., Ball, E. E., Ying, H., Forêt, S., Takahashi, S., Weynberg, K. D., van Oppen, M. J. H., Morrow, K., Chan, C. X., Rosic, N., Leggat, W., Sprungala, S., Imelfort, M., Tyson, G. W., ... Fyffe, T. (2015). The ReFuGe 2020 Consortium-using “omics” approaches to explore the adaptability and resilience of coral holobionts to environmental change. *Frontiers in Marine Science*, 2(SEP).
70. Wolanski, E., Richmond, R. H., & McCook, L. (2004). A model of the effects of land-based, human activities on the health of coral reefs in the Great Barrier Reef and in Fouha Bay, Guam, Micronesia. *Journal of Marine Systems*, 46(1–4), 133–144.
71. Wooldridge, S., Brodie, J., & Furnas, M. (2006). Exposure of inner-shelf reefs to nutrient enriched runoff entering the Great Barrier Reef Lagoon: Post-European changes and the design of water quality targets. *Marine Pollution Bulletin*, 52(11), 1467–1479.
72. Xia, X., Zhang, S., Li, S., Zhang, L., Wang, G., Zhang, L., Wang, J. and Li, Z. (2018). The cycle of nitrogen in river systems: sources, transformation, and flux. *Environmental Science: Processes & Impacts*, 20(6), 863–891.

Supplementary Material

Read Count Table (post-filtering):

Oceanic Clade		Riverine Clade		Distant Clade	
Sample	Reads	Sample	Reads	Sample	Reads
OIL09	5,949	OIL13	7,650	OFL04	445,467
ORL32	9,798	RFL17	5,788	OFL06	366,550
OTL05	6,280	RFL19	5,061	OFL07	384,069
OTL07	9,668	RTL21	5,752	OFL08	278,279
OFL12	173,488	OFL22	73,481	OFL30	111,579
OFL18	2,609,943	OFL36	1,370,717	OIL10	24,437
OFL24	229,850	OIL04	78,511	OIL11	183,434
OFL32	118,804	OIL12	122,652	OIL14	633,810
OFL33	237,853	ORL07	224,662	OIL19	367,642
OIL01	76,532	RFL04	3,321,333	OIL21	565,815
OIL03	163,865	RFL07	949,799	OIL22	348,707
OIL05	140,036	RFL08	516,632	OIL25	207,419
OIL20	130,837	RFL09	300,348	OIL26	359,277
OIL24	12,297	RFL11	10,140	OIL29	97,079
OIL33	333,738	RFL14	510,257	OIL32	454,428
OIL40	366,611	RFL15	736,432	ORL01	77,332
ORL03	68,613	RFL18	115,039	ORL02	13,077
ORL04	47,641	RFL20	131,172	ORL17	75,140
ORL05	159,820	RFL21	77,691	ORL31	76,220
ORL06	113,155	RFL22	301,512	ORL38	91,280
ORL08	270,565	RFL23	113,543	OTL21	458,471
ORL09	186,081	RFL24	56,138	OTL35	61,622
ORL10	118,679	RFL25	158,945	OTL36	262,400
ORL12	55,200	RFL26	1,076,724	RFL16	55,685
ORL13	99,728	RFL27	23,333	RFL29	1,378,708
ORL14	107,569	RFL28	22,178	RIL10	80,874
ORL15	93,141	RFL30	225,540	RIL11	1,146,822
ORL16	57,249	RFL31	1,157,212	RTL13	86,364

Oceanic Clade (continued)		Riverine Clade (continued)		East Fore Reef Clade	
Sample	Reads	Sample	Reads	Sample	Reads
ORL18	789,598	RFL32	348,555	OIL15	132,948
ORL20	610,594	RFL33	1,153,141	OIL28	155,495
ORL21	742,012	RFL34	228,126	OIL35	474,255
ORL22	150,945	RFL36	1,471,697	ORL19	29,190
ORL26	109,721	RFL37	210,140	ORL39	24,450
ORL40	219,322	RFL39	65,662	OTL10	108,605
OTL01	175,403	RIL01	306,583	OTL19	730,860
OTL03	67,671	RIL02	27,027	OTL20	104,666
OTL04	59,118	RIL07	191,809	OTL26	57,055
OTL06	13,978	RIL08	90,582	OTL32	337,215
OTL08	32,021	RIL09	337,917	West Fore Reef Clade	
OTL09	50,952	RIL12	346,043	Sample	Reads
OTL15	49,035	RIL14	42,387	OFL01	7,362
OTL18	227,538	RIL15	128,958	OFL02	42,389
OTL23	60,117	RIL17	241,540	OFL03	30,286
OTL27	79,319	RIL24	123,645	OFL05	14,672
OTL29	651,933	RIL28	132,486	OFL23	153,227
OTL31	430,339	RIL36	10,519	OFL27	41,677
OTL34	29,837	RIL38	62,594	OFL34	74,046
RIL06	16,033	RTL01	341,865	OFL38	58,070
RIL18	573,888	RTL08	157,291	OTL24	108,522
RIL19	91,422	RTL09	182,622		
RIL21	26,899	RTL10	433,176		
RIL22	419,128	RTL11	287,674		
RIL23	44,657	RTL12	250,787		
RIL27	19,807	RTL15	210,486		
RIL29	323,919	RTL16	471,405		
RIL30	27,022	RTL17	117,452		
RIL31	52,919	RTL18	539,103		
RIL33	16,145	RTL20	150,558		
RTL07	138,336	RTL22	13,526		
RTL35	36,645	RTL23	73,024		
RTL36	287,071	RTL24	132,618		
		RTL25	145,519		
		RTL26	267,572		
		RTL33	134,544		

Abbreviations:

EFR = East Fore Reef

WFR = West Fore Reef

SD = Standard Deviation

CI = Confidence Interval

MLP= multiple location pair

SLP= single location pair

FR = Fore Reef

RD = River Delta

Sample Count and Percent Composition from Each Location						
Location	Oceanic	Riverine	Distant	EFR	WFR	SUM
Fouha	5 (10%)	29 (59%)	7 (14%)	0 (0%)	8 (16%)	49
Talofoto	18 (39%)	18 (39%)	4 (9%)	5 (11%)	1 (2%)	46
Inarajan	19 (38%)	16 (32%)	12 (24%)	3 (6%)	0 (0%)	50
Ritidian	19 (70%)	1 (4%)	5 (19%)	2 (7%)	0 (0%)	27

Table 1

Sample Count and Percent Composition of each Clade by geographic location					
Location	Oceanic	Riverine	Distant	EFR	WFR
Fouha	5 (8%)	29 (45%)	7 (25%)	0 (0%)	8 (89%)
Talofoto	18 (30%)	18 (28%)	4 (14%)	5 (50%)	1 (11%)
Inarajan	19 (31%)	16 (25%)	12 (43%)	3 (30%)	0 (0%)
Ritidian	19 (31%)	1 (2%)	5 (18%)	2 (20%)	0 (0%)
SUM	61	64	28	10	9

Table 2

Sample Count and Percent Composition from each environment						
Environment	Oceanic	Riverine	Distant	EFR	WFR	SUM
River Delta	14 (18%)	58 (75%)	5 (6%)	0 (0%)	0 (0%)	77 (45%)
Fore Reef	47 (49%)	6 (6%)	23 (24%)	10 (11%)	9 (9%)	95 (55%)

Table 3

Sample Count and Percent Composition of each clade from each environment					
Environment	Oceanic	Riverine	Distant	EFR	WFR
River Delta	14 (23%)	58 (91%)	5 (18%)	0 (0%)	0 (0%)
Fore Reef	47 (77%)	6 (9%)	23 (82%)	10 (100%)	9 (100%)
SUM	61	64	28	10	9

Table 4

Sample Count and Percent Abundance of Color Phenotype Across Clades						
Color	Oceanic	Riverine	Distant	EFR	WFR	SUM
Blue	2 (67%)	0 (0%)	0 (0%)	1 (33%)	0 (0%)	3
Purple	6 (40%)	0 (0%)	5 (33%)	0 (0%)	4 (27%)	15
Green	12 (60%)	8 (40%)	0 (0%)	0 (0%)	0 (0%)	20
Yellow	24 (41%)	19 (33%)	12 (21%)	3 (5%)	0 (0%)	58
Cream	2 (50%)	2 (50%)	0 (0%)	0 (0%)	0 (0%)	4
Brown	13 (21%)	32 (51%)	8 (13%)	5 (8%)	5 (8%)	63

Table 5

Sample Count and Percent Composition of Color Phenotype by Clade					
Color	Oceanic	Riverine	Distant	EFR	WFR
Blue	2 (3%)	0 (0%)	0 (0%)	1 (11%)	0 (0%)
Purple	6 (10%)	0 (0%)	5 (20%)	0 (0%)	4 (44%)
Green	12 (20%)	8 (13%)	0 (0%)	0 (0%)	0 (0%)
Yellow	24 (41%)	19 (31%)	12 (48%)	3 (33%)	0 (0%)
Cream	2 (3%)	2 (3%)	0 (0%)	0 (0%)	0 (0%)
Brown	13 (22%)	32 (52%)	8 (32%)	5 (56%)	5 (56%)
SUM	59	61	25	9	9

Table 6

Single Location and Multiple Location Clonal Pairs by Clade and Site															
	Eastern Populations									Western Populations					
	Talofofo				Inarajan					Fouha				Ritidian	
Clade	SLP	Triplet	RD Samples	FR Samples	SLP	MLP	Triplet	RD Samples	FR Samples	SLP	MLP	RD Samples	FR Samples	MLP	FR Samples
Riverine	2	0	4	0	1	2	0	2	2	0	1	1	0	1	1
Distant	0	0	0	0	0	0	0	0	0	1	0	1	1	0	0
EFR	0	1	0	3	0	0	0	0	0	0	0	0	0	0	0
Oceanic	2	0	0	4	0	1	1	1	3	0	0	0	0	1	1

Table 7: Clonal pairs and triplets in each massive *Porites* clade.

Single Location and Multiple Location Highly Related Sample Pairs												
	Eastern Populations								Western Populations			
	Talofofo				Inarajan				Ritidian			
Clade	SLP	MLP	RD Samples	FR Samples	SLP	MLP	RD Samples	FR Samples	SLP	MLP	FR Samples	
Riverine	0	1	1	0	1	1	2	1	0	0	0	
Oceanic	0	1	0	1	0	0	0	0	1	1	3	

Table 8: Closely related pairs in each massive *Porites* clade

<u>GenoDive AMOVA</u>									
Source of Variation	Nested In	% Variation	F-Stat	F-value	SD	CI (2.5%)	CI (97.5%)	P-value	F'-value
Within Individual	--	0.337	F_it	0.663	0.002	0.658	0.668	--	--
Among Individual	Population	0.055	F_is	0.140	0.002	0.136	0.144	0.001	--
Among Population	--	0.608	F_st	0.608	0.003	0.603	0.613	0.001	0.642

Table 9: All clade genomic dataset AMOVA

<u>GenoDive AMOVA</u>									
Source of Variation	Nested In	% Variation	F-Stat	F-value	SD	CI (2.5%)	CI (97.5%)	P-value	F'-value
Within Individual	--	0.845	F_it	0.155	0.003	0.149	0.162	--	--
Among Individual	Population	0.138	F_is	0.140	0.003	0.134	0.147	0.001	--
Among Population	--	0.018	F_st	0.018	0.001	0.016	0.019	0.001	0.019

Table 10: Riverine Clade AMOVA

GenoDive AMOVA									
Source of Variation	Nested In	% Variation	F-Stat	F-value	SD	CI (2.5%)	CI (97.5%)	P-value	F'-value
Within Individual	--	0.839	F_it	0.161	0.004	0.153	0.169	--	--
Among Individual	Population	0.118	F_is	0.123	0.004	0.115	0.131	0.001	--
Among Population	--	0.043	F_st	0.043	0.002	0.040	0.046	0.001	0.045

Table 11: Oceanic Clade AMOVA

GenoDive AMOVA									
Source of Variation	Nested In	% Variation	F-Stat	F-value	SD	CI (2.5%)	CI (97.5%)	P-value	F'-value
Within Individual	--	0.817	F_it	0.183	0.005	0.173	0.192	--	--
Among Individual	Population	0.103	F_is	0.112	0.005	0.102	0.122	0.001	--
Among Population	--	0.080	F_st	0.080	0.002	0.075	0.085	0.001	0.102

Table 12: Distant Clade AMOVA

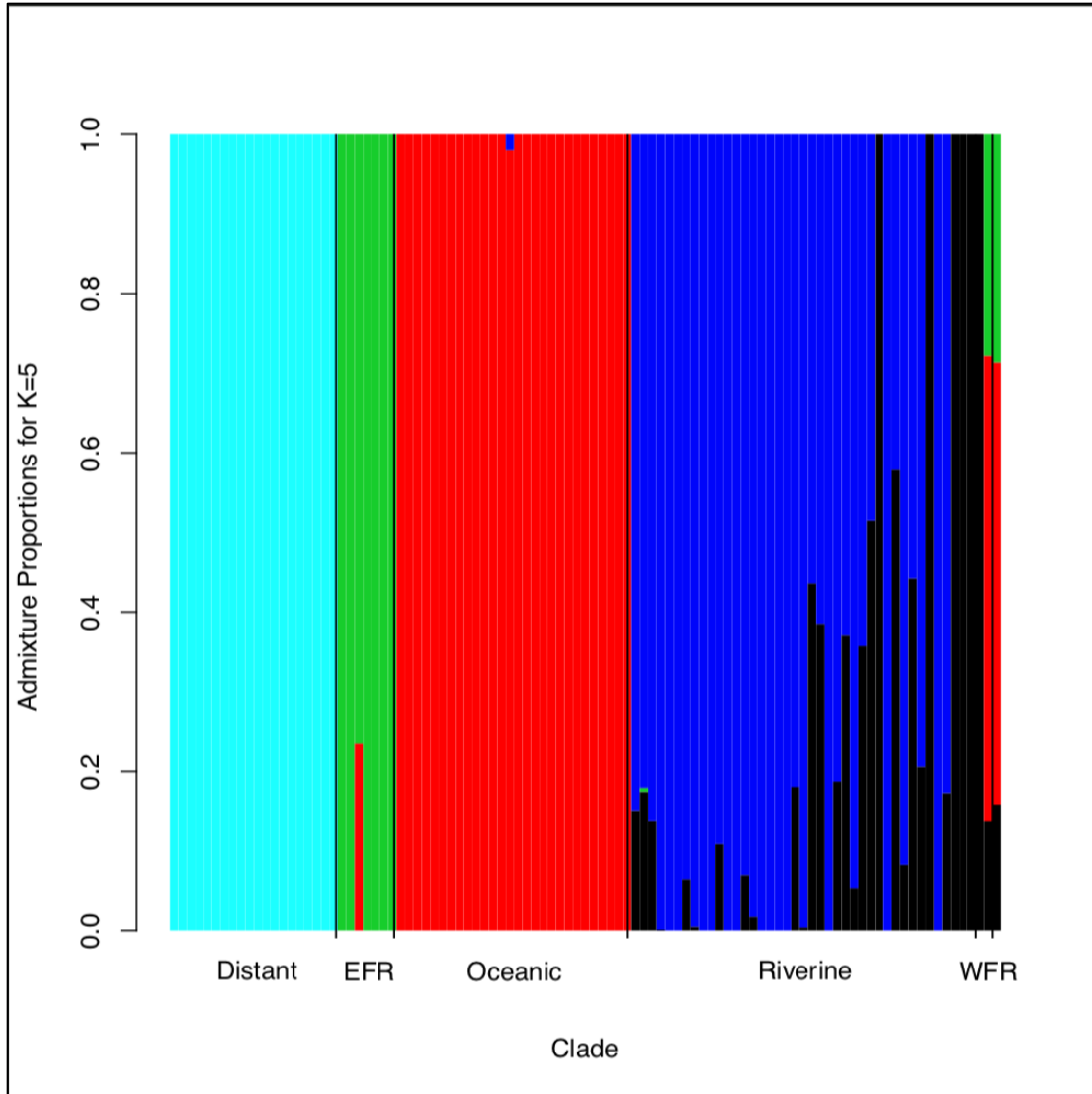


Figure 4: K=5 NGSAdmix plot

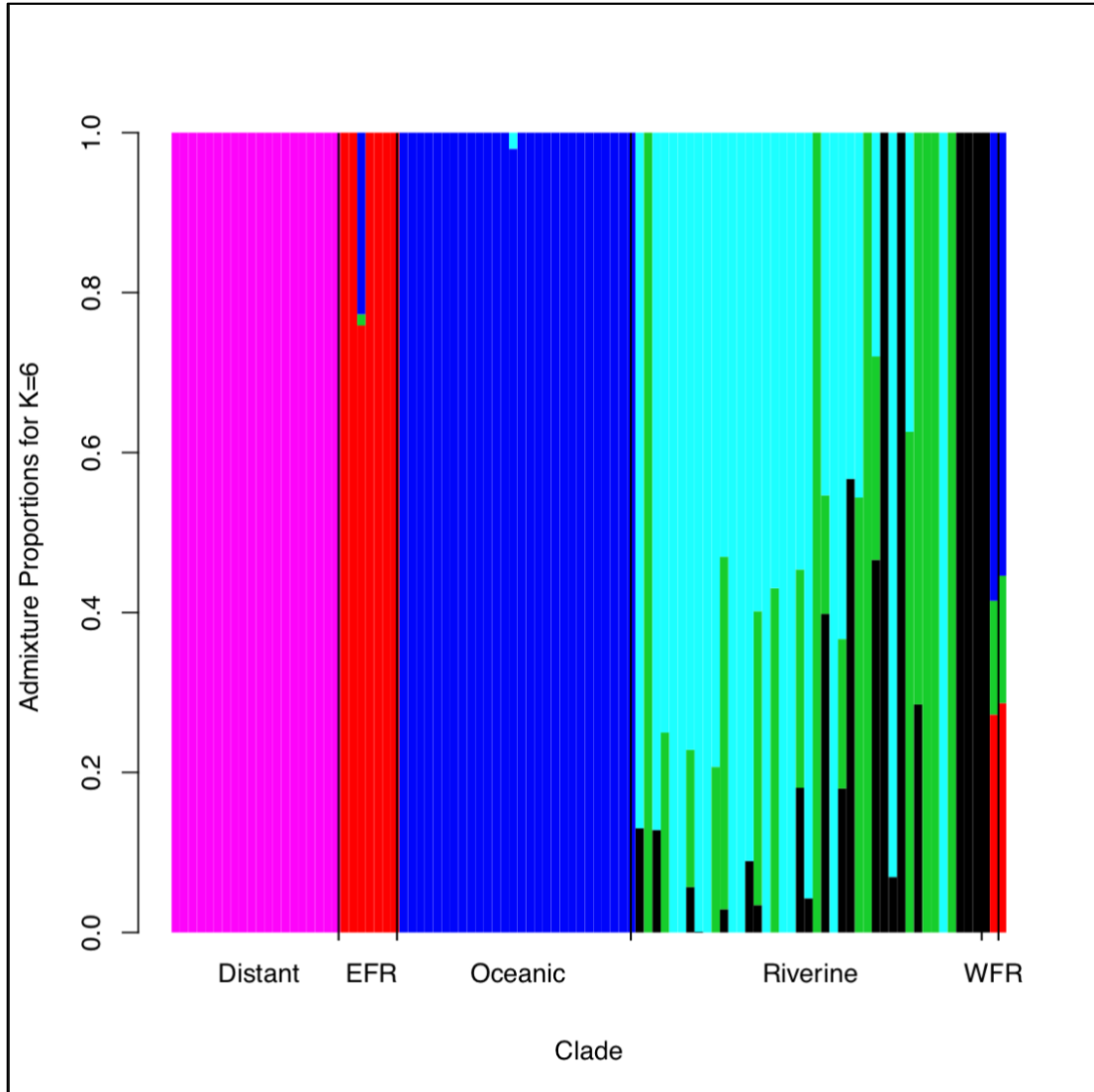


Figure 5: K=6 NGSAdmix plot